

DreamInsert: Zero-Shot Image-to-Video Object Insertion from A Single Image

Qi Zhao^{1,2} Zhan Ma¹ Pan Zhou²

¹Nanjing University ²Singapore Management University

qizhao@smail.nju.edu.cn mazhan@nju.edu.cn panzhou@smu.edu.sg

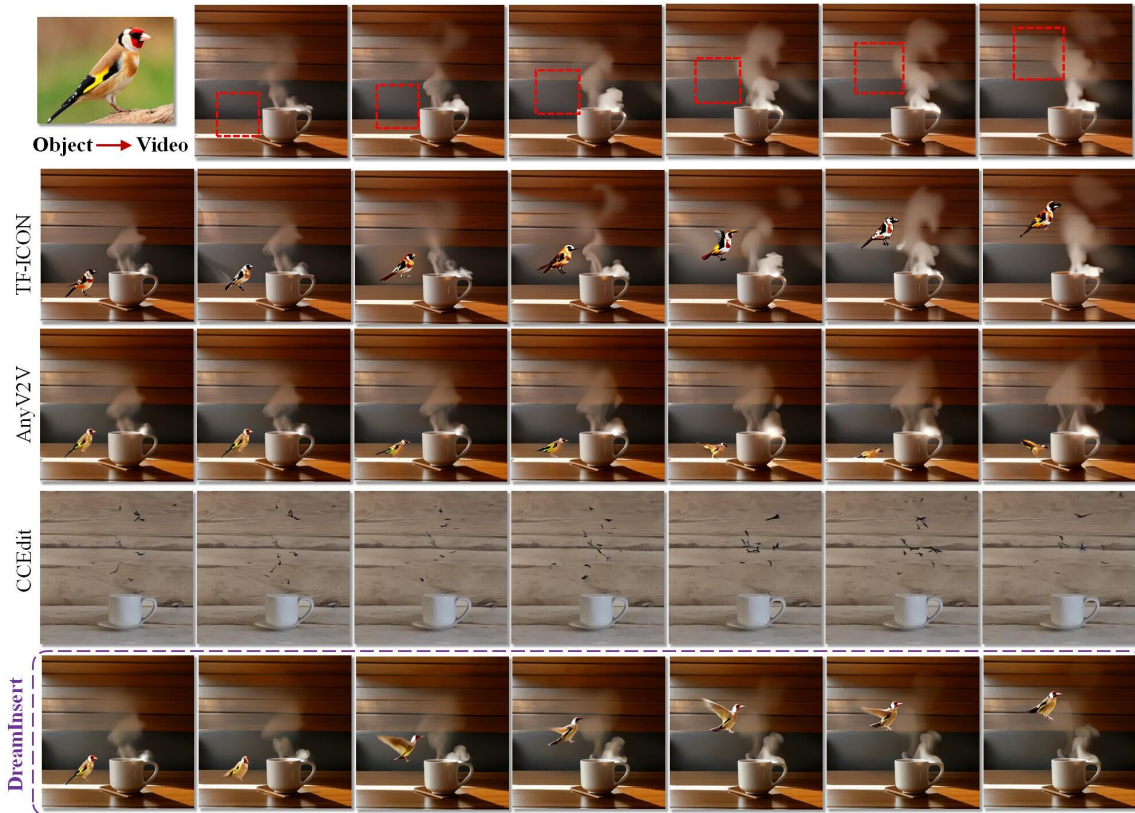


Figure 1. Visual examples on “Coffee-Bird”, where DreamInsert realizes zero-shot insertion for static object into dynamic video.

Abstract

Recent developments in generative diffusion models have turned many dreams into realities. For video object insertion, existing methods typically require additional information, such as a reference video or a 3D asset of the object, to generate the synthetic motion. However, inserting an object from a single reference photo into a target background video remains an uncharted area due to the lack of unseen motion information. We propose DreamInsert, which achieves Image-to-Video Object Insertion in a training-free manner for the first time. By incorporating the trajectory of the object into consideration, DreamInsert can predict the unseen

object movement, fuse it harmoniously with the background video, and generate the desired video seamlessly. More significantly, DreamInsert is both simple and effective, achieving zero-shot insertion without end-to-end training or additional fine-tuning on well-designed image-video data pairs. We demonstrated the effectiveness of DreamInsert through a variety of experiments, examples of which are shown in Fig. 1. Leveraging this capability, we present the first results for Image-to-Video object insertion in a training-free manner, paving exciting new directions for future content creation and synthesis. The code will be released soon.

1. Introduction

Memory and imagination are two fundamental functions of the human brain that play a crucial role in how we perceive our surroundings [1]. Humans can recall vivid scenes and reshape memories with imagined alterations, reflects the entanglement between memory and imagination. In practice, inserting an object into a video is a challenging task with applications in various fields such as film production [2], virtual reality [3], and therapeutic visualizations [4].

With recent progress in diffusion model [5–8], such as text conditional generation [9–13], image-to-video (I2V) generation [14, 15], and image/video editing [16–18], object insertion has shown impressive results across different scenarios, such as image-to-image (I2I) [18, 19], video-to-video (V2V) [20, 21], and object-to-3D (O23D) [22–24]. Each scenario presents unique challenges, such as ensuring multiview consistency in O23D or harmonizing style attributes like lighting and shadow in I2I tasks.

Despite these advances, *Image-to-Video (I2V) object insertion* remains an unexplored frontier. Formally, given a static object from a single image, how can we inject it into a dynamic video that aligns with background within desired movements? This I2V insertion task is particularly valuable for applications in fields like virtual reality and content creation [23, 25, 26], where realistic and adaptable object placements can greatly enhance user experience.

Challenges. The task of I2V insertion presents significant challenges in two key aspects. *First*, integrating a static object from an image into a dynamic video requires generating realistic motion that aligns with the object’s natural behavior. For instance, a dog can run but cannot fly. Unlike I2I and O23D which do not impose constraints on motion and V2V that benefits from a reference motion, I2V insertion is inherently ill-posed. The absence of a direct motion reference creates ambiguity—there are infinitely many plausible ways an object might behave within a video.

Challenge 1: Lack of reference motion when inserting a static object into a dynamic video.

Second, even after generating motion for the inserted object, maintaining both spatial and temporal consistency across video frames is a formidable challenge. When a static object is introduced into a background video, discrepancies in movement, positioning, and object-background interactions can cause unnatural distortions. Ensuring the seamless integration of the object while preserving environmental coherence is a key differentiator between I2V insertion and other video synthesis tasks like I2V or T2V generation. More critically, modeling optimal object-environment interactions through supervised learning or fine-tuning is nearly infeasible. Data pairs depicting the same object exhibiting various behaviors in identical scenes are virtually non-existent. Furthermore, training on imbalanced object-video distributions risks severe mode collapse [27], limiting

the model’s ability to generalize across diverse scenarios.

Challenge 2: The generated object motion must maintain both spatiotemporal and environmental consistency.

Contributions. To address these challenges, we introduce **DreamInsert**, a novel zero-shot I2V insertion framework that enables controllable and training-free object integration into videos via a two-stage process. To tackle Challenge 1, DreamInsert leverages textual descriptions and a predefined trajectory sequences as conditioning inputs to generate reasonable but coarse motion for the static object in the first stage. For Challenge 2, DreamInsert refines the generated motions in the second stage, ensuring spatiotemporal consistency and seamless environmental integration under the guidance of a pretrained generative model. By adopting a training-free paradigm, DreamInsert circumvents the need for costly model fine-tuning, enabling flexible and adaptive object insertion without requiring additional training data. Experimental results validate its effectiveness across a wide range of scenarios. For instance, visual examples of the “Coffee-Bird” are illustrated in Fig. 1.

- We introduce DreamInsert as the first training-free solution for I2V insertion, incorporating textual descriptions and a trajectory sequences as conditioning signals to generate realistic and non-existent object motions.
- Leveraging pretrained knowledge, DreamInsert achieves plausible object insertions without additional fine-tuning, effectively addressing the challenge of insufficient training data pairs.
- Through various experiments, we demonstrate DreamInsert’s ability to insert static objects into videos with diverse backgrounds while maintaining natural and coherent object-environment interactions.

2. Related work

Controllable Video Generation. The stability and efficiency of diffusion models [5–7] in density estimation have accelerated advances in content generation [10, 25, 28–35], enabling controllable video generation [12–17, 26, 36–68]. For controllable video generation, some researchers fine-tune text-to-image (T2I) models [10, 25] on multimodal data pairs [12, 13, 34] or customized datasets [17, 50], enabling Text-to-Video (T2V) generation. Other studies use motion vectors [55], Plücker embeddings for camera paths [52], and joint motion for camera-object relations [26] as condition signals for fine-grained control. Besides, subject-driven generation [17, 54, 69–71] is gradually emerging as a promising direction, aiming to generate consistent content tailored to specific subjects.

Training-free Content Editing. Some works fine-tune the backbone model for content editing [16, 62, 72–76], but may harm model’s generalization ability. Training-free methods offer a compelling alternative that uses noise inversion and feature injection for content editing [14, 62, 72–

86]. PtP [81] discovers the importance of cross-attention layers to control the relation between the image layout and words in the prompt. PnP [82] observes that the control of the generated content can be achieved by manipulating the spatial features and their self-attention. AnyV2V [77] divides the video editing task into first frame editing and I2V generation, leading to controllable video composition.

Some works aim to address the mismatch during inversion processes. Classifier-Free Guidance (CFG) [87] has been shown to have impacts on content fidelity [18, 84, 88]. SDEdit-based methods [75, 89–91] apply perturbations to pixels before inversion. Precise control over space and time remains a challenge in content editing.

Object Insertion. Research on object insertion has focused on image-based (I2I) and 3D scene insertion. For videos, the focus has been on rigid body insertion and light rendering, with limited work on predicting object dynamics. I2I methods [19, 92–94] often employ inpainting models to learn interactions between foreground and background. Training-free image composition approaches, such as [18], leverage powerful T2I diffusion models for object blending.

3D object insertion [22–24, 95, 96] involves integrating objects into 3D scenes, especially using Neural Radiance Fields (NeRF). Instruct-NeRF2NeRF [22] first uses text guidance for 3D editing and InSeRF [24] achieves rough object placement from single views. The main challenges in 3D insertion include multiview consistency and realistic rendering. In contrast, I2V insertion emphasizes generating unseen motion while maintaining consistency.

3. Preliminary

We introduce the preliminary of Latent Diffusion Model (LDM) and DDIM inversion which being pivotal in the DreamInsert, to better illustrate the proposed pipeline.

Latent Diffusion Model. LDM is used in models of both coarse injection and spatiotemporal alignment stages. In LDM, input images z_0 will be encoded in latents space as z_0 by VAE. This pixel compression process saves computational costs while maintaining semantic features, and also helps improve the diversity and editability of diffusion model generation [97, 98]. During forward process, the encoded latents z_0 will be perturbed by noise into z_t :

$$z_t = \sqrt{\bar{\alpha}_t} z_0 + \sqrt{1 - \bar{\alpha}_t} \epsilon, \quad \epsilon \sim \mathcal{N}(0, I),$$

where $\bar{\alpha}_t$ determines the noise strength according to step t . During the denoising process, the noise patterns will be modeled via a noise prediction model s_θ with conditional signal c by minimizing the training objective:

$$\arg \min \mathbb{E}_{z_0, \epsilon \sim \mathcal{N}(0, I), t, c} [\|\epsilon - s_\theta(z_0, t, c)\|].$$

Once the training is completed, new images can be decoded

by gradually denoising the samples from $p(z)$,

$$z_{t-1} = \sqrt{\frac{\bar{\alpha}_{t-1}}{\bar{\alpha}_t}} z_t + \left(\sqrt{\frac{1}{\bar{\alpha}_{t-1}} - 1} - \sqrt{\frac{1}{\bar{\alpha}_t} - 1} \right) \cdot s_\theta(z_t, t, c).$$

Inversion-based Editing. When we obtain the score model s_θ , we can achieve the mapping between noise and image through inversion. Specifically, we can use DDIM [7] inversion to obtain the corresponding noise latents,

$$z_{t+1} = \sqrt{\frac{\bar{\alpha}_{t+1}}{\bar{\alpha}_t}} z_t + \left(\sqrt{\frac{1}{\bar{\alpha}_{t+1}} - 1} - \sqrt{\frac{1}{\bar{\alpha}_t} - 1} \right) \cdot s_\theta(z_t, t, c).$$

Once we obtain the inverted latent representation for the images or video frames, we can modify those content by manipulating the latents, adding new conditions, and feature injection, namely *Inversion-based Editing* [75, 77, 81, 82, 84, 99, 100].

4. DreamInsert

Fig. 2 illustrates the overall framework of DreamInsert, structured as a two-stage process to systematically address the two challenges of I2V insertion. Sec. 4.1 provides an overview of the framework which consists of two stages. The first stage, Motion Creation, is detailed in Sec. 4.2, while the second stage, Spatiotemporal Alignment, is described in Sec. 4.3.

4.1. Overall Framework

As discussed earlier, I2V insertion faces two fundamental challenges: (1) the absence of reference motion for static objects and (2) the need for spatiotemporal consistency to ensure seamless integration into a dynamic video. To tackle these challenges, we decompose the object’s motion into two hierarchical components: coarse- and fine-grained motions. The former defines the overall movement direction and speed of the object while keeping the coarse-grained appearance of object, while the later ensures the realism of the object’s appearance, maintains spatiotemporal coherence, and adapts to the surrounding environment.

To generate coarse-grained motion, we leverage a predefined (bounding box level) movement trajectory and textual descriptions as conditioning signals together with the static image to generate a sequence of plausible coarse motion trajectories. This forms Stage 1 of DreamInsert, addressing Challenge 1. Next, Stage 2 resolves Challenge 2 and refines coarse-grained motion into a fine-grained motion via a pretrained I2V model, ensuring both object integrity and environmental consistency. The core motivation behind this two-stage design is that I2V insertion requires a delicate balance between preserving background fidelity and synthesizing realistic object motion—a challenge that cannot be effectively handled through one-shot generation.

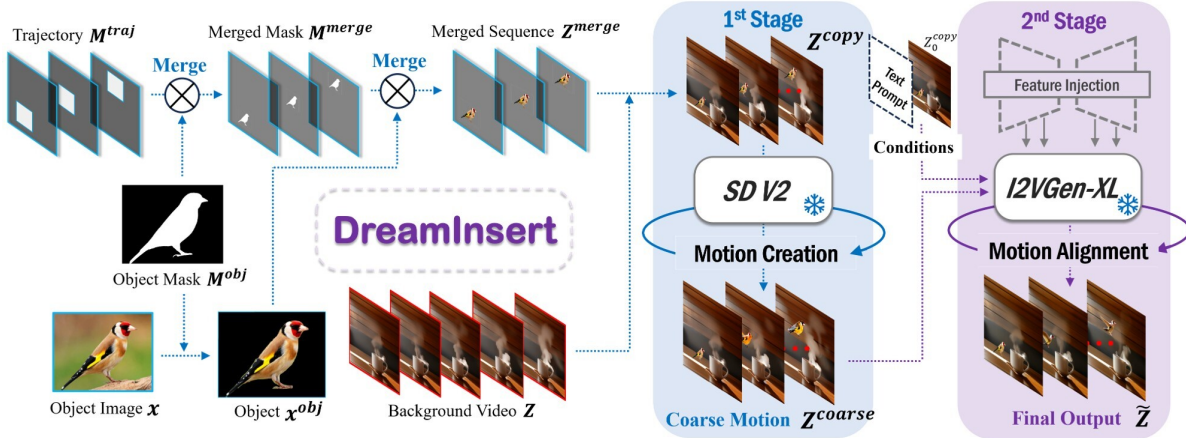


Figure 2. The overview of DreamInsert where Merge denotes the rescale + replace operation and $\mathbf{Z}^{\text{merge}} = \text{Merge}(\mathbf{x}^{\text{obj}}, \mathbf{M}^{\text{merge}})$, showcasing two stages: the blue part is the first stage of motion creation, while the purple part is the second stage of spatiotemporal alignment.

4.2. First-stage: Motion Creation

Here we study how to use object image \mathbf{x} , background video \mathbf{Z} , and trajectory sequence \mathbf{M}^{traj} to generate a coarse-grained motion of the object. This coarse-grained motion can be obtained by a frame-wise merging operation and can be further refined in the subsequent stage for consistency.

As shown in Fig. 2, for a static object in the reference image \mathbf{x} , we use a predefined bounding-box (bbox) sequence \mathbf{M}^{traj} to control its movement trajectory, where \mathbf{M}^{traj} has the same sequence length as the background video \mathbf{Z} . Each frame in \mathbf{M}^{traj} contains a bbox that indicates the expected position of the object, where pixels within the object area are set to 1 and the rest are set to 0. This sequence provides guidance for objects’ movement.

To generate the coarse-grained motion for object by using \mathbf{M}^{traj} , we use Segment Anything 2 [101], a segmentation model, to extract the object segmentation mask \mathbf{M}^{obj} as shown in Fig. 2. Then we resize \mathbf{M}^{obj} to fit the bbox in \mathbf{M}^{traj} for replacement, yielding a frame-specific merged mask:

$$\mathbf{M}_i^{\text{merge}} = \text{Merge}(\mathbf{M}_i^{\text{obj}}, \mathbf{M}_i^{\text{traj}}), \quad i \in [0, N]$$

where $\mathbf{M}_i^{\text{merge}}$ is the merged mask of the i -th frame. As shown in Fig. 2, Merge denotes the operation that resize the object mask \mathbf{M}^{obj} to the same shape of the bbox in $\mathbf{M}_i^{\text{traj}}$ and then replace it, forming a merged mask. Consequently, we first segment the object \mathbf{x}^{obj} from the image \mathbf{x} using \mathbf{M}^{obj} , $\mathbf{x}^{\text{obj}} = \mathbf{x} \odot \mathbf{M}^{\text{obj}}$, where \odot denotes the Hadamard product, i.e., element-wise product. Then, we resize and copy the \mathbf{x}^{obj} according to $\mathbf{M}_i^{\text{merge}}$ into the corresponding background frame \mathbf{Z}_i and obtain $\mathbf{Z}_i^{\text{copy}}$,

$$\mathbf{Z}_i^{\text{copy}} = \text{Merge}(\mathbf{x}^{\text{obj}}, \mathbf{M}_i^{\text{merge}}) + \mathbf{Z}_i \odot (1 - \mathbf{M}_i^{\text{merge}}).$$

Then to create coarse-grained motion, we explore two approaches: pixel noise injection and latent noise injection. While the former is straightforward and computationally ef-

ficient, the latter, which leverages diffusion inversion, often delivers superior results as shown in Sec. 5.

Pixel Noise Injection. To generate motion for static objects efficiently, we introduce a lightweight Pixel Noise Injection (PN-Inj) that selectively perturbs key regions while preserving the background. We obtain the coarse motion sequence $\mathbf{Z}^{\text{coarse}}$ by adding less Gaussian noise $\epsilon \sim \mathcal{N}(0, 1)$ to the object and more Gaussian noise into its interaction areas in each video frame, while keeping the background area fixed. A visual representation of this region division is shown in Fig. 3 (left). For each frame $\mathbf{Z}_i^{\text{copy}}$, we apply different noise intensities to different regions:

$$\begin{aligned} \mathbf{Z}_i^{\text{coarse}} = & \mathbf{Z}_i^{\text{copy}} \odot (1 - \mathbf{M}_i^{\text{traj}}) && \text{(background: no noise)} \\ & + \sigma_1 * \epsilon \odot \mathbf{M}_i^{\text{IA}} + (1 - \sigma_1) * \mathbf{Z}_i^{\text{copy}} \odot \mathbf{M}_i^{\text{IA}} && \text{(interaction: more noise)} \\ & + \sigma_2 * \epsilon \odot \mathbf{M}_i^{\text{merge}} + (1 - \sigma_2) * \mathbf{Z}_i^{\text{copy}} \odot \mathbf{M}_i^{\text{merge}}, && \text{(object: less noise)} \end{aligned}$$

where \oplus is XOR operation and $\mathbf{M}_i^{\text{IA}} = \mathbf{M}_i^{\text{merge}} \oplus \mathbf{M}_i^{\text{traj}}$ denotes the interaction (IA) area as shown in Fig. 3 (left). σ_1 and σ_2 control noise intensity of interaction and object area, respectively.

After applying different noise injection strategies, in the second stage we will refine the coarse video $\mathbf{Z}^{\text{coarse}}$ using a text-to-video diffusion model. Similar to image editing techniques [75, 81, 82], injecting noise into specific regions of a video frame enables targeted modifications based on input conditions, such as textual descriptions in this work. Additionally, higher noise levels provide greater flexibility for editing. Given the image-to-video nature of our task and the need for controlled editing, we apply different noise intensities to distinct regions. First, since the object is initially static in each frame $\mathbf{Z}_i^{\text{copy}}$, it must be modified to exhibit motion while preserving its appearance, requiring noise injection for editing. Second, the interaction region between the object and the scene requires significant editing and thus needs stronger noise injection, as inserting a new object alters occlusion, lighting, and shadows. Lastly, the

background should remain unchanged to maintain visual fidelity, and thus should get rid of noise injection. By following this strategy, lower noise levels facilitate natural object motion generation, higher noise levels allow for more extensive interaction modifications, and the absence of noise in the background ensures consistency with the original scene. **Latent Noise Injection.** While Pixel Noise Injection (PN-Inj) efficiently generates a coarse-grained motion sequence that captures the approximate appearance and position of an object, real-world applications often require finer control guided by textual descriptions. To address this, we introduce latent noise injection (LN-Inj) which injects noise into the latent representation of video inversion, enabling the generation of more natural object interactions and motion under text guidance during the denoising process of a text-to-image model.

To achieve this, we employ inversion-based editing to incorporate the textual condition \mathcal{C}^{obj} into \mathbf{Z}^{copy} for coarse-grained motion generation. Specifically, we obtain the inverted noise representation, a.k.a., latent representation, by using SDv2 [25], an Ordinary Differential Equation (ODE)-based inversion method with DPM++ [102] for text-to-image generation:

$$\xi_i = \text{Inv}_I(\mathbf{Z}_i^{\text{copy}}). \quad (1)$$

This latent representation ξ_i allow the reconstruction of the original input video frames through multiple denoising steps in SDv2 (see Sec. 3). Moreover, same as image editing techniques [75, 81, 82], injecting noise into specific regions of the video frame enables targeted modifications, ensuring that the edited regions align with the input conditions, such as the provided text description.

Since the newly inserted object does not naturally blend with the original background frame, we introduce Gaussian noise $\epsilon \sim \mathcal{N}(0, 1)$ into the interaction area (IA) of the latent representations ξ_i . This encourages the model to synthesize harmonious interactions from a new starting point $\hat{\xi}_i$:

$$\hat{\xi}_i = \xi_i \odot (1 - \mathbf{m}_i^{\text{IA}}) + \epsilon \odot \mathbf{m}_i^{\text{IA}},$$

where \mathbf{m}_i^{IA} represents the rescaled mask of \mathbf{M}_i^{IA} in the latent space, and \mathbf{M}_i^{IA} is the interaction area in the original frame space. Fig. 3 visualizes this process, where ‘‘Injected Latent’’ is the $\hat{\xi}_i$ and the colored region is the \mathbf{m}_i^{IA} .

Finally, the refined frame $\mathbf{Z}_i^{\text{coarse}}$, which includes improved motion synthesis, is generated using the decoder Dec_I of the text-to-image (T2I) model, guided by the textual description \mathcal{C}^{obj} :

$$\mathbf{Z}_i^{\text{coarse}} = \text{Dec}_I(\{\hat{\xi}_i\}, \mathcal{C}^{\text{obj}}), \quad i \in [0, N].$$

Compared with pixel noise injection, this latent noise injection uses the extra textual description \mathcal{C}^{obj} , and often provides better coarse-grained motion and also the final image-to-video insertion performance as shown in Sec. 5.

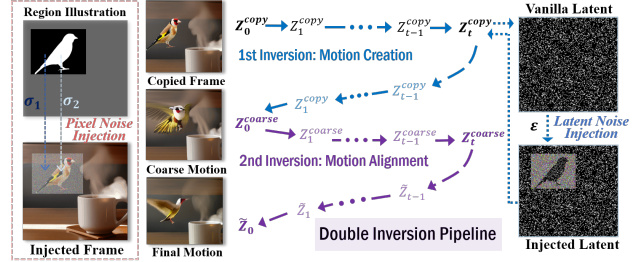


Figure 3. *Left*: Pixel noise injection with the region illustration, where gray for the background, white for the object area and black for the interaction (IA) area. *Right*: The overview of Double Inversion pipeline with latent noise injection. We only add noise in the latent’s IA area and obtain coarse frame after denoising.



Figure 4. Existing training-based subject-driven method can hardly maintain consistency in scenarios of disordering semantic.

4.3. Second-stage: Spatiotemporal Alignment

The first stage generates a coarse video, $\mathbf{Z}^{\text{coarse}}$, which provides an initial motion sequence for the inserted object. However, $\mathbf{Z}^{\text{coarse}}$ often exhibits inconsistencies in both object appearance and its interaction with the background across frames, such as unnatural bird flight motions, as illustrated in Fig. 5 (top). To address this, the second stage refines $\mathbf{Z}^{\text{coarse}}$ for spatiotemporal coherence while preserving realistic object-background interactions.

Moreover, such disordering semantic cases are rare in real-world datasets, making it infeasible to fine-tune backbone models for improved performance. Subject-driven adaptation methods [17, 54, 69–71] struggle with this limitation, failing to maintain both fidelity and consistency. Fig. 4 visualizes the inconsistencies produced by VideoBooth [54] in such scenarios.

Challenges for Spatiotemporal Consistency. Existing video generation models [15, 35, 44, 54, 58] are typically trained on large-scale text-image [103, 104] or text-video datasets [35, 105, 106], allowing them to learn general semantic relationships between text prompts and natural scenes. However, due to the ill-posed nature of image-to-video (I2V) object insertion, the synthesized video often deviates significantly from the videos in the training dataset. The inserted object may appear in unexpected contexts (e.g., a bird in an indoor scene with a coffee cup and ta-



Figure 5. Visual examples of outputs in two stages. *Top*: motion creation in the 1st stage; *Bottom*: alignment in the 2nd stage.

ble, as shown in Fig. 4), leading to rare and even novel scenarios. This semantic mismatch is a primary cause of spatiotemporal inconsistencies, making it difficult for existing models to generate fine-grained motion which is Challenge 2 as discussed in Sec. 1. Moreover, those rare and even novel video scenarios are hard to collect in reality and may not exist, making it challenging to finetune the backbone model to generate fine-grained motion. Owing to the lack of data, existing subject-driven methods [17, 54, 69–71] can hardly handle this situation, unable to maintain fidelity and consistency. Different results using VideoBooth [54] are visualized in Fig. 4.

Training-Free Editing. To overcome these challenges, we leverage the pretrained generative model’s spatiotemporal knowledge in a training-free manner. Our approach decouples the synthesis process into two steps. The background is reconstructed using the inverted latents of the coarse video, mitigating semantic mismatches between the inserted object and the scene. The textual prompt is used exclusively to refine the object’s motion while ensuring seamless integration during the denoising process.

Given the coarse motion sequence, the copied object from the first frame, and a textual description, DreamInsert performs inversion-based editing to guide the denoising process toward a high-fidelity, temporally coherent output. Specifically, the coarse video $\mathbf{Z}^{\text{coarse}}$ is first inverted into the latent space of an I2V model via DDIM inversion [7]:

$$\zeta = \text{Inv}_V(\mathbf{Z}^{\text{coarse}}), \quad (2)$$

where ζ represents the latent representation. Next, using the first frame of the inserted object $\mathbf{Z}_0^{\text{copy}}$ and textual alignment prompt $\mathcal{C}^{\text{align}}$, the I2V model [15] performs controlled denoising to generate the spatiotemporally aligned video:

$$\tilde{\mathbf{Z}} = \mathbf{Z}^{\text{align}} = \text{Dec}_V(\zeta, \mathbf{Z}_0^{\text{copy}}, \mathcal{C}^{\text{align}}). \quad (3)$$

This ensures that the inserted object blends naturally with the background while maintaining temporal coherence.

Feature Injection. To further refine spatiotemporal alignment, we introduce feature and attention score injection during the early denoising steps inspired by [77, 82]. These techniques preserve crucial motion cues and prevent drift during the refinement process. Specifically, during the DDIM inversion in the 2^{nd} stage, the attention score is injected performed in the first 5 steps out of the total denoising

step of 50 which guides the reconstruction of the inserted object and maintains spatial consistency. Moreover, we perform spatial feature injection in the first 5 steps to preserve the vanilla coarse movement and also reinforce motion continuity. By injecting coarse movement information from the initial video, these techniques ensure the final output maintains both realism and fidelity while preserving the object’s intended motion.

Discussions. As shown in Fig. 3, we refer to this two-stage inversion-based refinement pipeline as Double Inversion (D-Inv), contrasting it with PN-Inj, as it enables the insertion of static objects into dynamic videos through two-stage inversion-based editing. Unlike prior methods, D-Inv achieves seamless I2V insertion without additional finetuning or training data, and shows strong robustness across diverse object-background combinations. Accordingly, D-Inv is set as the default pipeline for DreamInsert.

5. Experiments

We conducted comprehensive experiments to verify the effectiveness of DreamInsert. The main results contain quantitative and qualitative evaluations in Sec. 5.2 and Sec. 5.3. User study is given in Sec. 5.4 and ablation study in Sec. 5.5. More details and results are demonstrated in the Appendix.

5.1. Settings.

To verify the performance of different methods on I2V insertion, we propose a dataset, I2V Insertion (I2VIns), and all experiments were conducted on I2VIns in an NVIDIA L40S GPU.

I2V Insertion Dataset. I2VIns dataset contains 14 object-video pairs used for evaluation, each case has a background video, an object image and a trajectory sequence. For background videos, six of them are from DAVIS16 [107] and the others are generated by AnimateDiff [50] using text prompts. MotionLora [50] is used to control camera movement in some of them and all prompts for the background videos please refer to the Appendix. Each background video contains 16 frames with the shape 512×512 , which covers various scenes from indoor to outdoor. Objects’ images are collected from the Internet. For each object-video pairs, we use a b-box sequence as the trajectory to control the movement of the object.

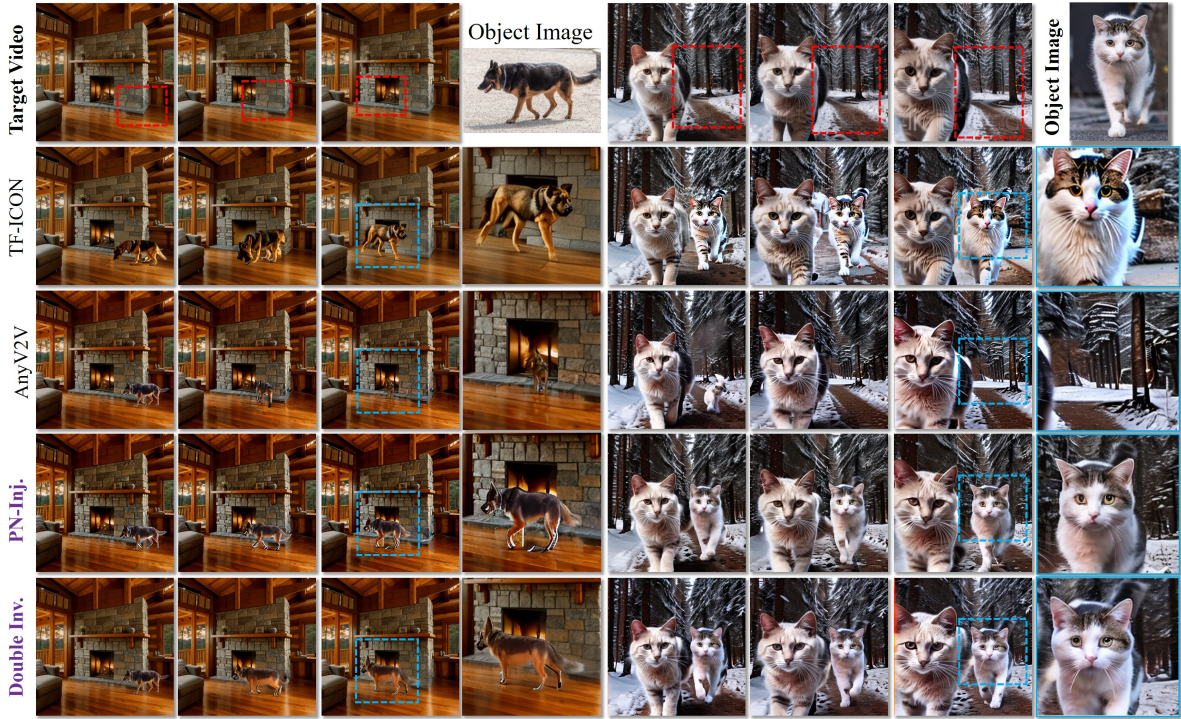


Figure 6. Visual comparison of DreamInsert with other methods, showing results at the 2nd, 8th, and 16th frames (from left to right).

Metrics. To quantitatively evaluate the synthesis results, we used different metrics. We use Clip-I [108] and DINO [109] score to evaluate the fidelity of insertion results, and Clip-T [108] to evaluate the degree of text matching. In addition, we propose an Adv-Viclip score to evaluate the overall quality of the results.

Baselines. We select some of the latest content editing methods to compare with DreamInsert. *TF-ICON* [18] is one of the SOTA image editing methods, and we use it for frame-wise object insertion. *CCEdit* [74] is a generalized video editing method trained on large-scale video datasets [106] using a T2I model as backbone. *AnyV2V* [77] is a training-free video editing method that enables zero-shot editing of various downstream tasks.

5.2. Quantitative Evaluation

Fidelity. We use Clip-I score [108] to calculate the similarity between the copied sequence and prediction to validate the *background* fidelity. Besides, we use DINO score [109] to calculate distance between object image and the b-box area of each synthesized frame to assess the *object* fidelity. Results are shown in Tab. 1, DreamInsert achieves the best result of 91.77 in D-Inv setting.

Text-Matching. We calculate Clip Text (Clip-T) [108] score between each model’s output and conditional prompt, thereby gauging the accuracy of the created motions instructed by the text. DreamInsert obtained the motion which is more in line with the prompt description.

Overall Quality by Adversarial Evaluation. Compared

	AnyV2V	CCEdit	TF-ICON	PN-Inj.	D-Inv.
Clip-I Score	88.72	72.19	90.19	91.49	91.77
DINO Score	0.645	0.534	0.735	0.743	0.751
Clip-T Score	26.75	24.13	26.67	26.89	26.84
Adv-Viclip Score	0.483	0.322	0.762	0.747	0.812

Table 1. Quantitative Comparison in various metrics.

to frame-wise fidelity, overall consistency is more important for a video and has a greater impact on the visual experience. Inspired by VBench [110], we use Viclip [105] to assess the overall consistency. Due to the specific nature of the insertion task, it is inaccurate to solely calculate the distance between prompts and outputs, as the background video may already match the information in the prompt. For example, in “Winter-Cat”, the background video inherently contains semantic information about “cat walking”. Even if the model fails to insert the object, the output video may still receive a high prompt-matching score.

Therefore, for each object-video pair and its optimal prompt, we designed a fake prompt, forming an adversarial library consisting of 28 prompts (e.g., “One cat walks towards the camera” as the fake prompt and “Two cats walk towards the camera” as the optimal one). Viclip will calculate the distance between each output and all prompts in the library. The probability value of the optimal prompt is used as the final result, namely *Adversarial Viclip* (*Adv-Viclip*) score. Results are given in Tab. 1 where D-Inv demonstrates significant advantages (0.483 \rightarrow 0.812, 68% improvement against AnyV2V). For all the prompts, discussions and more details, please refer to Appendix.

5.3. Qualitative Evaluation

Shown in Fig. 6, we provide visual examples to compare DreamInsert with baseline methods. The results of CCEdit are given in the Appendix, as it failed to insert object into the video. On the left of Fig. 6 is the “Cabin-Dog”, which contains a background video about a cabin with wooden floors and a burning fireplace. The object is a German Shepherd dog and the trajectory is in linear movement. All methods uses “A german shepherd walking on the floor” as the text prompt. Although the dog in the output of AnyV2V shows motions that align with the action of “walk” in the prompt, it violates the real-world logic where the dog walks into the burning fireplace. The results generated by DreamInsert-D-Inv achieve superior consistency in both spatial appearance and temporal movement, leading to reasonable environmental interaction.

On the right, “Winter-Cat” represents a more challenging case where the inserted cat occupies the main body of the frames and the position of the b-box remains almost unchanged, containing few movement information. DreamInsert achieves superior visual results due to its good text-matching ability. However, AnyV2V and CCEdit failed to insert the object correctly, and TF-ICON was unable to maintain spatial or temporal consistency.

5.4. User Study

Moreover, we provide a detailed user study, where 20 users rated 5 aspects (**Fidelity** of the inserted object, **Smoothness** of the generated object motion, **Interaction** with the background, the **Text-Matching** quality, and the overall **Quality**) on 7 videos and give a rating from 1 to 5 (ranging from failed, poor, fair, good, to excellent). For each aspect, we propose a question, and users respond to it by ratings. For example, for Fidelity, the question is: “Is the object in the synthesized video consistent with the object in the reference image?”. Please refer to Appendix for more details.

Tab. 2 shows the average score of different methods in those aspects, where DreamInsert achieves significant improvements. For overall quality, PN-Inj and D-Inv achieve 65.1% and 86.3% improvements compared to AnyV2V, which has the best performance among the baselines. D-Inv acquires a 16.8% gain (3.33 \rightarrow 3.89) towards PN-Inj and 78.4% gain toward AnyV2V (2.18 \rightarrow 3.89) on the reasonable *interaction*. For the average rating, D-Inv achieves a 77.0% gain (2.26 \rightarrow 4.00) towards AnyV2V and a 11.4% gain (3.59 \rightarrow 4.00) towards PN-Inj.

	AnyV2V	CCEdit	TF-ICON	PN-Inj.	D-Inv.
Fidelity	2.73	1.30	2.22	3.84	4.06
Smoothness	2.11	1.24	2.18	3.59	4.07
Interaction	2.18	1.21	1.98	3.33	3.89
Text-matching	2.14	1.23	2.35	3.69	4.04
Quality	2.12	1.24	2.09	3.50	3.95
Average	2.26	1.24	2.16	3.59	4.00

Table 2. User study comparison with the maximum score being 5.

5.5. Ablation Study

We perform ablation studies towards the noise scale added in PN-Inj and the feature injection steps in the 2nd stage. Results are shown in Fig. 7 and Fig. 8, and more studies are given in the Appendix.

Noise scale in PN-Inj. We discussed how the noise scale affects the performance of PN-Inj (Eqn. 4.2). As shown in Fig. 7, we set $\sigma_1=0.4$ and $\sigma_2=0.1$ as the default setting which in bold font. If σ_1 is set too high, $\sigma_1=1.0$ in the right-bottom, it prevents the region from generating reasonable interactions, while a too small $\sigma_1=0.2$ (right-top), will result in the diversity vanishing and the region not being able to generate motions. Setting the noise scale in the object area too high ($\sigma_2=0.5$) will cause distortion.



Figure 7. Ablation study on scale of noise added in PN-Inj, where σ_1 for the interaction area and σ_2 for the object area.

Feature injection. We discussed the impact of the injection steps in D-Inv. In Fig. 8 of “Library-Batman”, the numbers from left to right represent the first few steps of injection: spatial feature, spatial attention score, and temporal attention score, of the total of 50 denoising steps. Fig. 8 shows that an early stop of feature and score injection will harm the fidelity, while more steps may result in the object vanishing or blurring.



Figure 8. Ablation study on feature injection steps.

6. Conclusion

We introduce DreamInsert, a novel framework for Image-to-Video Insertion, achieving this task in a training-free manner for the first time. Leveraging object trajectory and textual guidance, DreamInsert generates realistic motion and seamlessly integrates objects into background videos. Various experiments validate its effectiveness, marking a significant step forward in video content creation and opening new directions for future research in video synthesis.

Limitations. DreamInsert relies on I2V generative models for spatiotemporal alignment which is essential for insertion. However, current I2V models struggle with highly

complex scenes like intricate limb movements, often leading to inconsistencies. As a result, DreamInsert inherits these limitations, facing challenges in handling such complex scenarios effectively.

References

- [1] Sinéad L Mullally and Eleanor A Maguire. Memory, imagination, and predicting the future. *Neuroscientist*, 2014. 2
- [2] Hongda Jiang, Xi Wang, Marc Christie, Libin Liu, and Baoquan Chen. Cinematographic camera diffusion model. *Comput. Graph. Forum*, 2024. 2, 6
- [3] Kalman Glanz, Albert Rizzo, and Graap Ken. Virtual reality for psychotherapy: Current reality and future possibilities. *Psychotherapy: Theory, Research, Practice, Training*, 2003. 2
- [4] Maria Matsangidou, Boris Otkhmezuri, Chee Siang Ang, Marios N. Avraamides, Giuseppe Riva, Andrea Gaggioli, Despoina Iosif, and Maria Karekla. "now i can see me" designing a multi-user virtual reality remote psychotherapy for body weight and shape concerns. *Hum. Comput. Interact.*, 2022. 2, 6
- [5] Jascha Sohl-Dickstein, Eric A. Weiss, Niru Maheswaranathan, and Surya Ganguli. Deep unsupervised learning using nonequilibrium thermodynamics. In Francis R. Bach and David M. Blei, editors, *Proceedings of the 32nd International Conference on Machine Learning, ICML 2015*, 2015. 2
- [6] Jonathan Ho, Ajay Jain, and Pieter Abbeel. Denoising diffusion probabilistic models. In Hugo Larochelle, Marc'Aurelio Ranzato, Raia Hadsell, Maria-Florina Balcan, and Hsuan-Tien Lin, editors, *Advances in Neural Information Processing Systems 33: Annual Conference on Neural Information Processing Systems 2020*, 2020.
- [7] Jiaming Song, Chenlin Meng, and Stefano Ermon. Denoising diffusion implicit models. In *9th International Conference on Learning Representations, ICLR 2021*, 2021. 2, 3, 6
- [8] black-forest labs. Flux.1-dev. In <https://huggingface.co/black-forest-labs/FLUX.1-dev>, 2024. 2
- [9] Chitwan Saharia, William Chan, Saurabh Saxena, Lala Li, Jay Whang, Emily L. Denton, Seyed Kamyar Seyed Ghasemipour, Raphael Gontijo Lopes, Burcu Karagol Ayan, Tim Salimans, Jonathan Ho, David J. Fleet, and Mohammad Norouzi. Photorealistic text-to-image diffusion models with deep language understanding. In *Advances in Neural Information Processing Systems 35: Annual Conference on Neural Information Processing Systems 2022, NeurIPS 2022*, 2022. 2
- [10] Dustin Podell, Zion English, Kyle Lacey, Andreas Blattmann, Tim Dockhorn, Jonas Müller, Joe Penna, and Robin Rombach. SDXL: improving latent diffusion models for high-resolution image synthesis. In *The Twelfth International Conference on Learning Representations, ICLR 2024*, 2024. 2
- [11] Patrick Esser, Sumith Kulal, Andreas Blattmann, Rahim Entezari, Jonas Müller, Harry Saini, Yam Levi, Dominik Lorenz, Axel Sauer, Frederic Boesel, Dustin Podell, Tim Dockhorn, Zion English, and Robin Rombach. Scaling rectified flow transformers for high-resolution image synthesis. In *Forty-first International Conference on Machine Learning, ICML 2024*, 2024.
- [12] Andreas Blattmann, Robin Rombach, Huan Ling, Tim Dockhorn, Seung Wook Kim, Sanja Fidler, and Karsten Kreis. Align your latents: High-resolution video synthesis with latent diffusion models. In *IEEE/CVF Conference on Computer Vision and Pattern Recognition, CVPR 2023*, 2023. 2
- [13] Uriel Singer, Adam Polyak, Thomas Hayes, Xi Yin, Jie An, Songyang Zhang, Qiyuan Hu, Harry Yang, Oran Ashual, Oran Gafni, Devi Parikh, Sonal Gupta, and Yaniv Taigman. Make-a-video: Text-to-video generation without text-video data. In *The Eleventh International Conference on Learning Representations, ICLR 2023*, 2023. 2
- [14] Wenqi Ouyang, Yi Dong, Lei Yang, Jianlou Si, and Xingang Pan. I2vedit: First-frame-guided video editing via image-to-video diffusion models. *CoRR*, abs/2405.16537, 2024. 2
- [15] Shiwei Zhang, Jiayu Wang, Yingya Zhang, Kang Zhao, Hangjie Yuan, Zhiwu Qin, Xiang Wang, Deli Zhao, and Jingren Zhou. I2vgen-xl: High-quality image-to-video synthesis via cascaded diffusion models. *CoRR*, abs/2311.04145, 2023. 2, 5, 6
- [16] Lvmin Zhang, Anyi Rao, and Maneesh Agrawala. Adding conditional control to text-to-image diffusion models. In *IEEE/CVF International Conference on Computer Vision, ICCV 2023*, 2023. 2
- [17] Nataniel Ruiz, Yuanzhen Li, Varun Jampani, Yael Pritch, Michael Rubinstein, and Kfir Aberman. Dreambooth: Fine tuning text-to-image diffusion models for subject-driven generation. In *IEEE/CVF Conference on Computer Vision and Pattern Recognition, CVPR 2023*, 2023. 2, 5, 6
- [18] Shilin Lu, Yanzhu Liu, and Adams Wai-Kin Kong. TF-ICON: diffusion-based training-free cross-domain image composition. In *IEEE/CVF International Conference on Computer Vision, ICCV 2023*, 2023. 2, 3, 7, 8, 9, 10, 11, 12, 13, 14, 15
- [19] Lingxiao Lu, Jiangtong Li, Junyan Cao, Li Niu, and Liqing Zhang. Painterly image harmonization using diffusion model. In *Proceedings of the 31st ACM International Conference on Multimedia, MM 2023*, 2023. 2, 3
- [20] Donghoon Lee, Tomas Pfister, and Ming-Hsuan Yang. Inserting videos into videos. In *IEEE Conference on Computer Vision and Pattern Recognition, CVPR 2019*, 2019. 2
- [21] Chen Bai, Zeman Shao, Guoxiang Zhang, Di Liang, Jie Yang, Zhuorui Zhang, Yujian Guo, Chengzhang Zhong, Yiqiao Qiu, Zhendong Wang, Yichen Guan, Xiaoyin Zheng, Tao Wang, and Cheng Lu. Anything in any scene: Photorealistic video object insertion. *CoRR*, 2024. 2
- [22] Ayaan Haque, Matthew Tancik, Alexei A. Efros, Aleksander Holynski, and Angjoo Kanazawa. Instruct-nerf2nerf: Editing 3d scenes with instructions. In *IEEE/CVF International Conference on Computer Vision, ICCV 2023*, 2023. 2, 3, 1

- [23] Ruofan Liang, Zan Gojic, Merlin Nimier-David, David Acuna, Nandita Vijaykumar, Sanja Fidler, and Zian Wang. Photorealistic object insertion with diffusion-guided inverse rendering. *CoRR*, abs/2408.09702, 2024. 2
- [24] Mohamad Shahbazi, Liesbeth Claessens, Michael Niemeyer, Edo Collins, Alessio Tonioni, Luc Van Gool, and Federico Tombari. Insef: Text-driven generative object insertion in neural 3d scenes. *CoRR*, abs/2401.05335, 2024. 2, 3, 1
- [25] Robin Rombach, Andreas Blattmann, Dominik Lorenz, Patrick Esser, and Björn Ommer. High-resolution image synthesis with latent diffusion models. In *IEEE/CVF Conference on Computer Vision and Pattern Recognition, CVPR 2022*, 2022. 2, 5, 6
- [26] Zhouxia Wang, Ziyang Yuan, Xintao Wang, Yaowei Li, Tianshui Chen, Menghan Xia, Ping Luo, and Ying Shan. Motionctrl: A unified and flexible motion controller for video generation. In Andres Burbano, Denis Zorin, and Wojciech Jarosz, editors, *ACM SIGGRAPH 2024 Conference Papers, SIGGRAPH 2024*, 2024. 2
- [27] Yiming Qin, Huangjie Zheng, Jiangchao Yao, Mingyuan Zhou, and Ya Zhang. Class-balancing diffusion models. *2023 IEEE/CVF Conference on Computer Vision and Pattern Recognition (CVPR)*, 2023. 2
- [28] Ian J. Goodfellow, Jean Pouget-Abadie, Mehdi Mirza, Bing Xu, David Warde-Farley, Sherjil Ozair, Aaron C. Courville, and Yoshua Bengio. Generative adversarial networks. *CoRR*, abs/1406.2661, 2014. 2
- [29] Aaron van den Oord, Oriol Vinyals, and Koray Kavukcuoglu. Neural discrete representation learning. In Isabelle Guyon, Ulrike von Luxburg, Samy Bengio, Hanna M. Wallach, Rob Fergus, S. V. N. Vishwanathan, and Roman Garnett, editors, *Advances in Neural Information Processing Systems 30: Annual Conference on Neural Information Processing Systems 2017*, 2017.
- [30] Patrick Esser, Robin Rombach, and Björn Ommer. Taming transformers for high-resolution image synthesis. In *IEEE Conference on Computer Vision and Pattern Recognition, CVPR 2021*, 2021.
- [31] Tero Karras, Samuli Laine, and Timo Aila. A style-based generator architecture for generative adversarial networks. In *IEEE Conference on Computer Vision and Pattern Recognition, CVPR 2019*, 2019.
- [32] Alexander Quinn Nichol, Prafulla Dhariwal, Aditya Ramesh, Pranav Shyam, Pamela Mishkin, Bob McGrew, Ilya Sutskever, and Mark Chen. GLIDE: towards photorealistic image generation and editing with text-guided diffusion models. In Kamalika Chaudhuri, Stefanie Jegelka, Le Song, Csaba Szepesvári, Gang Niu, and Sivan Sabato, editors, *International Conference on Machine Learning, ICML 2022*, 2022.
- [33] Prafulla Dhariwal and Alexander Quinn Nichol. Diffusion models beat gans on image synthesis. In Marc Aurelio Ranzato, Alina Beygelzimer, Yann N. Dauphin, Percy Liang, and Jennifer Wortman Vaughan, editors, *Advances in Neural Information Processing Systems 34: Annual Conference on Neural Information Processing Systems 2021, NeurIPS 2021*, 2021.
- [34] Jonathan Ho, Tim Salimans, Alexey A. Gritsenko, William Chan, Mohammad Norouzi, and David J. Fleet. Video diffusion models. In Sanmi Koyejo, S. Mohamed, A. Agarwal, Danielle Belgrave, K. Cho, and A. Oh, editors, *Advances in Neural Information Processing Systems 35: Annual Conference on Neural Information Processing Systems 2022, NeurIPS 2022*, 2022. 2
- [35] Andreas Blattmann, Tim Dockhorn, Sumith Kulal, Daniel Mendelevitch, Maciej Kilian, Dominik Lorenz, Yam Levi, Zion English, Vikram Voleti, Adam Letts, Varun Jampani, and Robin Rombach. Stable video diffusion: Scaling latent video diffusion models to large datasets. *CoRR*, abs/2311.15127, 2023. 2, 5
- [36] Zhiwu Qing, Shiwei Zhang, Jiayu Wang, Xiang Wang, Yujie Wei, Yingya Zhang, Changxin Gao, and Nong Sang. Hierarchical spatio-temporal decoupling for text-to-video generation. In *IEEE/CVF Conference on Computer Vision and Pattern Recognition, CVPR 2024*, 2024. 2
- [37] Omer Bar-Tal, Hila Chefer, Omer Tov, Charles Herrmann, Roni Paiss, Shiran Zada, Ariel Ephrat, Junhwa Hur, Yuanzhen Li, Tomer Michaeli, Oliver Wang, Deqing Sun, Tali Dekel, and Inbar Mosseri. Lumiere: A space-time diffusion model for video generation. *CoRR*, abs/2401.12945, 2024.
- [38] William Peebles and Saining Xie. Scalable diffusion models with transformers. In *IEEE/CVF International Conference on Computer Vision, ICCV 2023*, 2023.
- [39] Nanye Ma, Mark Goldstein, Michael S. Albergo, Nicholas M. Boffi, Eric Vanden-Eijnden, and Saining Xie. Sit: Exploring flow and diffusion-based generative models with scalable interpolant transformers. *CoRR*, abs/2401.08740, 2024.
- [40] Xiang Wang, Shiwei Zhang, Han Zhang, Yu Liu, Yingya Zhang, Changxin Gao, and Nong Sang. Videolcm: Video latent consistency model. *CoRR*, abs/2312.09109, 2023.
- [41] Xin Ma, Yaohui Wang, Gengyun Jia, Xinyuan Chen, Ziwei Liu, Yuan-Fang Li, Cunjian Chen, and Yu Qiao. Latte: Latent diffusion transformer for video generation. *CoRR*, abs/2401.03048, 2024.
- [42] Yash Jain, Anshul Nasery, Vibhav Vineet, and Harkirat S. Behl. Peekaboo: Interactive video generation via masked-diffusion. In *IEEE/CVF Conference on Computer Vision and Pattern Recognition, CVPR 2024*, 2024.
- [43] Wenyi Hong, Ming Ding, Wendi Zheng, Xinghan Liu, and Jie Tang. Cogvideo: Large-scale pretraining for text-to-video generation via transformers. In *The Eleventh International Conference on Learning Representations, ICLR 2023*, 2023.
- [44] Jonathan Ho, William Chan, Chitwan Saharia, Jay Whang, Ruiqi Gao, Alexey A. Gritsenko, Diederik P. Kingma, Ben Poole, Mohammad Norouzi, David J. Fleet, and Tim Salimans. Imagen video: High definition video generation with diffusion models. *CoRR*, abs/2210.02303, 2022. 5
- [45] Agrim Gupta, Lijun Yu, Kihyuk Sohn, Xiuye Gu, Meera Hahn, Li Fei-Fei, Irfan Essa, Lu Jiang, and José Lezama. Photorealistic video generation with diffusion models. *CoRR*, abs/2312.06662, 2023.

- [46] Jing Shi, Wei Xiong, Zhe Lin, and Hyun Joon Jung. Instant-booth: Personalized text-to-image generation without test-time finetuning. In *IEEE/CVF Conference on Computer Vision and Pattern Recognition, CVPR 2024*, 2024.
- [47] Bohao Peng, Jian Wang, Yuechen Zhang, Wenbo Li, Ming-Chang Yang, and Jiaya Jia. Controlnext: Powerful and efficient control for image and video generation. *CoRR*, abs/2408.06070, 2024.
- [48] Ben Poole, Ajay Jain, Jonathan T. Barron, and Ben Mildenhall. Dreamfusion: Text-to-3d using 2d diffusion. In *The Eleventh International Conference on Learning Representations, ICLR 2023*, 2023.
- [49] Yujie Wei, Shiwei Zhang, Hangjie Yuan, Xiang Wang, Haonan Qiu, Rui Zhao, Yutong Feng, Feng Liu, Zhizhong Huang, Jiaxin Ye, Yingya Zhang, and Hongming Shan. Dreamvideo-2: Zero-shot subject-driven video customization with precise motion control, 2024.
- [50] Yuwei Guo, Ceyuan Yang, Anyi Rao, Zhengyang Liang, Yaohui Wang, Yu Qiao, Maneesh Agrawala, Dahua Lin, and Bo Dai. Animatediff: Animate your personalized text-to-image diffusion models without specific tuning. In *The Twelfth International Conference on Learning Representations, ICLR 2024*, 2024. 2, 6, 1
- [51] Pengyang Ling, Jiazi Bu, Pan Zhang, Xiaoyi Dong, Yuhang Zang, Tong Wu, Huaian Chen, Jiaqi Wang, and Yi Jin. Motionclone: Training-free motion cloning for controllable video generation. *CoRR*, abs/2406.05338, 2024.
- [52] Hao He, Yinghao Xu, Yuwei Guo, Gordon Wetzstein, Bo Dai, Hongsheng Li, and Ceyuan Yang. Cameractrl: Enabling camera control for text-to-video generation. *CoRR*, abs/2404.02101, 2024. 2
- [53] Hu Ye, Jun Zhang, Sibao Liu, Xiao Han, and Wei Yang. Ip-adapter: Text compatible image prompt adapter for text-to-image diffusion models. *CoRR*, abs/2308.06721, 2023.
- [54] Yuming Jiang, Tianxing Wu, Shuai Yang, Chenyang Si, Dahua Lin, Yu Qiao, Chen Change Loy, and Ziwei Liu. Videobooth: Diffusion-based video generation with image prompts. In *IEEE/CVF Conference on Computer Vision and Pattern Recognition, CVPR 2024*, 2024. 2, 5, 6
- [55] Xiang Wang, Hangjie Yuan, Shiwei Zhang, Dayou Chen, Jiuniu Wang, Yingya Zhang, Yujun Shen, Deli Zhao, and Jingren Zhou. Videocomposer: Compositional video synthesis with motion controllability. In Alice Oh, Tristan Naumann, Amir Globerson, Kate Saenko, Moritz Hardt, and Sergey Levine, editors, *Advances in Neural Information Processing Systems 36: Annual Conference on Neural Information Processing Systems 2023, NeurIPS 2023*, 2023. 2
- [56] Hong Chen, Xin Wang, Guanning Zeng, Yipeng Zhang, Yuwei Zhou, Feilin Han, and Wenwu Zhu. Videodreamer: Customized multi-subject text-to-video generation with disen-mix finetuning. *CoRR*, abs/2311.00990, 2023.
- [57] Yuchao Gu, Yipin Zhou, Bichen Wu, Licheng Yu, Jia-Wei Liu, Rui Zhao, Jay Zhangjie Wu, David Junhao Zhang, Mike Zheng Shou, and Kevin Tang. Videoswap: Customized video subject swapping with interactive semantic point correspondence. In *IEEE/CVF Conference on Computer Vision and Pattern Recognition, CVPR 2024*, 2024.
- [58] Jay Zhangjie Wu, Yixiao Ge, Xintao Wang, Stan Weixian Lei, Yuchao Gu, Yufei Shi, Wynne Hsu, Ying Shan, Xiaohu Qie, and Mike Zheng Shou. Tune-a-video: One-shot tuning of image diffusion models for text-to-video generation. In *IEEE/CVF International Conference on Computer Vision, ICCV 2023*, 2023. 5
- [59] Yabo Zhang, Yuxiang Wei, Dongsheng Jiang, Xiaopeng Zhang, Wangmeng Zuo, and Qi Tian. Controlvideo: Training-free controllable text-to-video generation. In *The Twelfth International Conference on Learning Representations, ICLR 2024*, 2024.
- [60] Zhao Wang, Aoxue Li, Enze Xie, Lingting Zhu, Yong Guo, Qi Dou, and Zhenguo Li. Customvideo: Customizing text-to-video generation with multiple subjects. *CoRR*, abs/2401.09962, 2024.
- [61] Jiasong Feng, Ao Ma, Jing Wang, Bo Cheng, Xiaodan Liang, Dawei Leng, and Yuhui Yin. Fancyvideo: Towards dynamic and consistent video generation via cross-frame textual guidance. *CoRR*, abs/2408.08189, 2024.
- [62] Shaoteng Liu, Yuechen Zhang, Wenbo Li, Zhe Lin, and Jiaya Jia. Video-p2p: Video editing with cross-attention control. In *IEEE/CVF Conference on Computer Vision and Pattern Recognition, CVPR 2024*, 2024. 2
- [63] Haoxin Chen, Menghan Xia, Yingqing He, Yong Zhang, Xiaodong Cun, Shaoshu Yang, Jinbo Xing, Yaofang Liu, Qifeng Chen, Xintao Wang, Chao Weng, and Ying Shan. Videocrafter1: Open diffusion models for high-quality video generation. *CoRR*, abs/2310.19512, 2023.
- [64] Haoxin Chen, Yong Zhang, Xiaodong Cun, Menghan Xia, Xintao Wang, Chao Weng, and Ying Shan. Videocrafter2: Overcoming data limitations for high-quality video diffusion models. In *IEEE/CVF Conference on Computer Vision and Pattern Recognition, CVPR 2024*, 2024.
- [65] Cong Wang, Jiayi Gu, Panwen Hu, Songcen Xu, Hang Xu, and Xiaodan Liang. Dreamvideo: High-fidelity image-to-video generation with image retention and text guidance. *CoRR*, abs/2312.03018, 2023.
- [66] Xun Guo, Mingwu Zheng, Liang Hou, Yuan Gao, Yufan Deng, Pengfei Wan, Di Zhang, Yufan Liu, Weiming Hu, Zhengjun Zha, Haibin Huang, and Chongyang Ma. I2v-adapter: A general image-to-video adapter for diffusion models. In *ACM SIGGRAPH 2024 Conference Papers, SIGGRAPH 2024*, 2024.
- [67] Xiaoyu Shi, Zhaoyang Huang, Fu-Yun Wang, Weikang Bian, Dasong Li, Yi Zhang, Manyuan Zhang, Ka Chun Cheung, Simon See, Hongwei Qin, Jifeng Dai, and Hongsheng Li. Motion-i2v: Consistent and controllable image-to-video generation with explicit motion modeling. In Andres Burbano, Denis Zorin, and Wojciech Jarosz, editors, *ACM SIGGRAPH 2024 Conference Papers, SIGGRAPH 2024*, 2024.
- [68] Yaosi Hu, Chong Luo, and Zhenzhong Chen. Make it move: Controllable image-to-video generation with text descriptions. In *IEEE/CVF Conference on Computer Vision and Pattern Recognition, CVPR 2022*, 2022. 2
- [69] Miao Hua, Jiawei Liu, Fei Ding, Wei Liu, Jie Wu, and Qian He. Dreamtuner: Single image is enough for subject-driven generation. *ArXiv*, 2023. 2, 5, 6

- [70] Yu Zeng, Vishal M. Patel, Haochen Wang, Xun Huang, Ting-Chun Wang, Ming-Yu Liu, and Yogesh Balaji. Jedi: Joint-image diffusion models for finetuning-free personalized text-to-image generation. *2024 IEEE/CVF Conference on Computer Vision and Pattern Recognition (CVPR)*, 2024.
- [71] Wenhui Chen, Hexiang Hu, Yandong Li, Nataniel Ruiz, Xuhui Jia, Ming-Wei Chang, and William W. Cohen. Subject-driven text-to-image generation via apprenticeship learning. In *Advances in Neural Information Processing Systems 36: Annual Conference on Neural Information Processing Systems 2023, NeurIPS 2023*, 2023. 2, 5, 6
- [72] Omer Bar-Tal, Dolev Ofri-Amar, Rafail Fridman, Yoni Kasten, and Tali Dekel. Text2live: Text-driven layered image and video editing. In Shai Avidan, Gabriel J. Brostow, Moustapha Cissé, Giovanni Maria Farinella, and Tal Hassner, editors, *Computer Vision - ECCV 2022 - 17th European Conference, 2022*. 2
- [73] Patrick Esser, Johnathan Chiu, Parmida Atighehchian, Jonathan Granskog, and Anastasis Germanidis. Structure and content-guided video synthesis with diffusion models. In *IEEE/CVF International Conference on Computer Vision, ICCV 2023*, 2023.
- [74] Ruoyu Feng, Wenming Weng, Yanhui Wang, Yuhui Yuan, Jianmin Bao, Chong Luo, Zhibo Chen, and Baining Guo. Ccredit: Creative and controllable video editing via diffusion models. In *IEEE/CVF Conference on Computer Vision and Pattern Recognition, CVPR 2024*, 2024. 7, 2, 11, 12
- [75] Chenlin Meng, Yutong He, Yang Song, Jiaming Song, Jiajun Wu, Jun-Yan Zhu, and Stefano Ermon. Sdedit: Guided image synthesis and editing with stochastic differential equations. In *The Tenth International Conference on Learning Representations, ICLR 2022, 2022*. 3, 4, 5
- [76] Zheng Chong, Xiao Dong, Haoxiang Li, Shiyue Zhang, Wenqing Zhang, Xujie Zhang, Hanqing Zhao, and Xiaodan Liang. Catvton: Concatenation is all you need for virtual try-on with diffusion models. *CoRR*, abs/2407.15886, 2024. 2
- [77] Max Ku, Cong Wei, Weiming Ren, Harry Yang, and Wenhui Chen. Anyv2v: A plug-and-play framework for any video-to-video editing tasks. *CoRR*, abs/2403.14468, 2024. 3, 6, 7, 2, 8, 9, 10, 11, 12, 13, 14, 15
- [78] Jianhong Bai, Tianyu He, Yuchi Wang, Junliang Guo, Haoji Hu, Zuozhu Liu, and Jiang Bian. Uniedit: A unified tuning-free framework for video motion and appearance editing. *CoRR*, abs/2402.13185, 2024.
- [79] Jiaqi Guo, Sitong Su, Junchen Zhu, Lianli Gao, and Jingkuan Song. Training-free semantic video composition via pre-trained diffusion model. In *IEEE International Conference on Multimedia and Expo, ICME 2024*, 2024.
- [80] Wei Wang, Yaosen Chen, Yuegen Liu, Qi Yuan, Shubin Yang, and Yanru Zhang. MVOC: a training-free multiple video object composition method with diffusion models. *CoRR*, abs/2406.15829, 2024.
- [81] Amir Hertz, Ron Mokady, Jay Tenenbaum, Kfir Aberman, Yael Pritch, and Daniel Cohen-Or. Prompt-to-prompt image editing with cross-attention control. In *The Eleventh International Conference on Learning Representations, ICLR 2023*, 2023. 3, 4, 5
- [82] Narek Tumanyan, Michal Geyer, Shai Bagon, and Tali Dekel. Plug-and-play diffusion features for text-driven image-to-image translation. In *IEEE/CVF Conference on Computer Vision and Pattern Recognition, CVPR 2023*, 2023. 3, 4, 5, 6
- [83] Jian Hu, Jiayi Lin, Junchi Yan, and Shaogang Gong. Leveraging hallucinations to reduce manual prompt dependency in promptable segmentation. *CoRR*, abs/2408.15205, 2024.
- [84] Ron Mokady, Amir Hertz, Kfir Aberman, Yael Pritch, and Daniel Cohen-Or. Null-text inversion for editing real images using guided diffusion models. In *IEEE/CVF Conference on Computer Vision and Pattern Recognition, CVPR 2023*, 2023. 3
- [85] Rinon Gal, Yuval Alaluf, Yuval Atzmon, Or Patashnik, Amit Haim Bermano, Gal Chechik, and Daniel Cohen-Or. An image is worth one word: Personalizing text-to-image generation using textual inversion. In *The Eleventh International Conference on Learning Representations, ICLR 2023*, 2023.
- [86] Sihan Xu, Yidong Huang, Jiayi Pan, Ziqiao Ma, and Joyce Chai. Inversion-free image editing with natural language. *CoRR*, abs/2312.04965, 2023. 3
- [87] Jonathan Ho and Tim Salimans. Classifier-free diffusion guidance. *CoRR*, abs/2207.12598, 2022. 3
- [88] Bram Wallace, Akash Gokul, and Nikhil Naik. EDICT: exact diffusion inversion via coupled transformations. In *IEEE/CVF Conference on Computer Vision and Pattern Recognition, CVPR 2023*, 2023. 3
- [89] Jiteng Mu, Michaël Gharbi, Richard Zhang, Eli Shechtman, Nuno Vasconcelos, Xiaolong Wang, and Taesung Park. Editable image elements for controllable synthesis. In *Computer Vision - ECCV 2024 - 18th European Conference*, 2024. 3
- [90] Jaskirat Singh, Stephen Gould, and Liang Zheng. High-fidelity guided image synthesis with latent diffusion models. In *IEEE/CVF Conference on Computer Vision and Pattern Recognition, CVPR 2023*, 2023.
- [91] Duygu Ceylan, Chun-Hao Paul Huang, and Niloy J. Mitra. Pix2video: Video editing using image diffusion. In *IEEE/CVF International Conference on Computer Vision, ICCV 2023*, 2023. 3
- [92] Wenyan Cong, Jianfu Zhang, Li Niu, Liu Liu, Zhixin Ling, Weiyuan Li, and Liqing Zhang. Dovenet: Deep image harmonization via domain verification. In *2020 IEEE/CVF Conference on Computer Vision and Pattern Recognition, CVPR 2020*, 2020. 3
- [93] Mengwei Ren, Wei Xiong, Jae Shin Yoon, Zhixin Shu, Jianming Zhang, Hyunjoon Jung, Guido Gerig, and He Zhang. Relightful harmonization: Lighting-aware portrait background replacement. In *IEEE/CVF Conference on Computer Vision and Pattern Recognition, CVPR 2024*, 2024.
- [94] Nataniel Ruiz, Yuanzhen Li, Neal Wadhwa, Yael Pritch, Michael Rubinstein, David E. Jacobs, and Shlomi Fruchter. Magic insert: Style-aware drag-and-drop. *CoRR*, abs/2407.02489, 2024. 3

- [95] Ashkan Mirzaei, Tristan Aumentado-Armstrong, Marcus A. Brubaker, Jonathan Kelly, Alex Levinshtein, Konstantinos G. Derpanis, and Igor Gilitschenski. Reference-guided controllable inpainting of neural radiance fields. In *IEEE/CVF International Conference on Computer Vision, ICCV 2023*, 2023. 3
- [96] Yuhan Li, Yishun Dou, Yue Shi, Yu Lei, Xuanhong Chen, Yi Zhang, Peng Zhou, and Bingbing Ni. Focaldreamer: Text-driven 3d editing via focal-fusion assembly. In Michael J. Wooldridge, Jennifer G. Dy, and Sriraam Natarajan, editors, *Thirty-Eighth AAAI Conference on Artificial Intelligence, AAAI 2024*, 2024. 3, 1
- [97] Ciprian A. Corneanu, Raghudeep Gadde, and Aleix M. Martínez. Latentpaint: Image inpainting in latent space with diffusion models. In *IEEE/CVF Winter Conference on Applications of Computer Vision, WACV 2024*, 2024. 3
- [98] Seyedmorteza Sadat, Jakob Buhmann, Derek Bradley, Otmar Hilliges, and Romann M. Weber. CADs: unleashing the diversity of diffusion models through condition-annealed sampling. In *The Twelfth International Conference on Learning Representations, ICLR 2024*, 2024. 3
- [99] Xiang Wang, Shiwei Zhang, Hangjie Yuan, Zhiwu Qing, Biao Gong, Yingya Zhang, Yujun Shen, Changxin Gao, and Nong Sang. A recipe for scaling up text-to-video generation with text-free videos. In *IEEE/CVF Conference on Computer Vision and Pattern Recognition, CVPR 2024*, 2024. 3
- [100] Wenhao Li, Yichao Cao, Xiu Su, Xi Lin, Shan You, Mingkai Zheng, Yi Chen, and Chang Xu. Training-free long video generation with chain of diffusion model experts. *CoRR*, abs/2408.13423, 2024. 3
- [101] Nikhila Ravi, Valentin Gabeur, Yuan-Ting Hu, Ronghang Hu, Chaitanya Ryali, Tengyu Ma, Haitham Khedr, Roman Rädle, Chloé Rolland, Laura Gustafson, Eric Mintun, Junting Pan, Kalyan Vasudev Alwala, Nicolas Carion, Chao-Yuan Wu, Ross B. Girshick, Piotr Dollár, and Christoph Feichtenhofer. SAM 2: Segment anything in images and videos. *CoRR*, abs/2408.00714, 2024. 4
- [102] Cheng Lu, Yuhao Zhou, Fan Bao, Jianfei Chen, Chongxuan Li, and Jun Zhu. Dpm-solver++: Fast solver for guided sampling of diffusion probabilistic models. *CoRR*, 2022. 5
- [103] Christoph Schuhmann, Richard Vencu, Romain Beaumont, Robert Kaczmarczyk, Clayton Mullis, Aarush Katta, Theo Coombes, Jenia Jitsev, and Aran Komatsuzaki. LAION-400M: open dataset of clip-filtered 400 million image-text pairs. *CoRR*, abs/2111.02114, 2021. 5
- [104] Christoph Schuhmann, Romain Beaumont, Richard Vencu, Cade Gordon, Ross Wightman, Mehdi Cherti, Theo Coombes, Aarush Katta, Clayton Mullis, Mitchell Wortsman, Patrick Schramowski, Srivatsa Kundurthy, Katherine Crowson, Ludwig Schmidt, Robert Kaczmarczyk, and Jenia Jitsev. LAION-5B: an open large-scale dataset for training next generation image-text models. In *Advances in Neural Information Processing Systems 35: Annual Conference on Neural Information Processing Systems 2022, NeurIPS 2022*, 2022. 5
- [105] Yi Wang, Yinan He, Yizhuo Li, Kunchang Li, Jiashuo Yu, Xin Ma, Xinhao Li, Guo Chen, Xinyuan Chen, Yao-hui Wang, Ping Luo, Ziwei Liu, Yali Wang, Limin Wang, and Yu Qiao. Internvid: A large-scale video-text dataset for multimodal understanding and generation. In *The Twelfth International Conference on Learning Representations, ICLR 2024*, 2024. 5, 7, 3, 4
- [106] Max Bain, Arsha Nagrani, Gül Varol, and Andrew Zisserman. Frozen in time: A joint video and image encoder for end-to-end retrieval. In *2021 IEEE/CVF International Conference on Computer Vision, ICCV 2021*, 2021. 5, 7
- [107] Federico Perazzi, Jordi Pont-Tuset, Brian McWilliams, Luc Van Gool, Markus H. Gross, and Alexander Sorkine-Hornung. A benchmark dataset and evaluation methodology for video object segmentation. In *2016 IEEE Conference on Computer Vision and Pattern Recognition, CVPR 2016*, 2016. 6, 1, 5, 9, 11
- [108] Alec Radford, Jong Wook Kim, Chris Hallacy, Aditya Ramesh, Gabriel Goh, Sandhini Agarwal, Girish Sastry, Amanda Askell, Pamela Mishkin, Jack Clark, Gretchen Krueger, and Ilya Sutskever. Learning transferable visual models from natural language supervision. In Marina Meila and Tong Zhang, editors, *Proceedings of the 38th International Conference on Machine Learning, ICML 2021*, 2021. 7
- [109] Mathilde Caron, Hugo Touvron, Ishan Misra, Hervé Jégou, Julien Mairal, Piotr Bojanowski, and Armand Joulin. Emerging properties in self-supervised vision transformers. In *2021 IEEE/CVF International Conference on Computer Vision, ICCV 2021*, 2021. 7, 3
- [110] Ziqi Huang, Yinan He, Jiashuo Yu, Fan Zhang, Chenyang Si, Yuming Jiang, Yuanhan Zhang, Tianxing Wu, Qingyang Jin, Nattapol Chanpaisit, Yaohui Wang, Xinyuan Chen, Limin Wang, Dahua Lin, Yu Qiao, and Ziwei Liu. Vbench: Comprehensive benchmark suite for video generative models. In *IEEE/CVF Conference on Computer Vision and Pattern Recognition, CVPR 2024*, 2024. 7, 3
- [111] Jack Hessel, Ari Holtzman, Maxwell Forbes, Ronan Le Bras, and Yejin Choi. Clipscore: A reference-free evaluation metric for image captioning. In *Proceedings of the 2021 Conference on Empirical Methods in Natural Language Processing, EMNLP 2021*, 2021. 3
- [112] Lisa Bode. The uncanny valley. *The Animation Studies Reader*, 2019. 6
- [113] Suzanne Witterholt. Treating the trauma of rape: Cognitive-behavioral therapy for ptsd. *Psychiatric Services*, 1999. 6

DreamInsert: Zero-Shot Image-to-Video Object Insertion from A Single Image

Supplementary Material

1. Experiments Detail

1.1. I2VIns Dataset

To compare the performance of different methods and demonstrate the effectiveness of our approach on Image-to-Video (I2V) object insertion, we propose the **I2V Insertion (I2VIns)** Dataset, which containing 14 video-object pairs and each case includes a background video, an object image, and a pre-prepared trajectory.

Background Video. The background videos in the I2VIns dataset include both synthesized and real videos for a better evaluation of the insertion performance. Each background video contains 16 frames in the shape of 512×512 . 5 of the videos are from DAVIS16 [107], which are “Carround”, “Lucia”, “Crossing”, “Gold-fish”, “Dog-goose”. The rest of the videos are synthesized videos which are generated by AnimateDiff [50], and some of them using MotionLora to control the camera motion, such as “Hill-Horse” and “Winter-Cat”. The corresponding prompts for each background video are as follows:

- Cabin-Dog: “A rustic cabin living room with a stone fireplace and animal skins.”
- Coffee-Bird: “A steaming cup of coffee on a wooden table, with the aroma and steam creating a warm, inviting atmosphere.”
- Forest-Horse: “The scene transitions to a lush, green forest, with birds chirping and leaves rustling in the breeze, raw photo, beautiful shadow, hyperrealism, ultra high res, 4K.”
- Hill-Horse: “Yellow wildflowers gently swaying in the breeze, rolling hills, clear blue sky, river, 8k uhd, soft lighting, high quality.” (MotionLora: “PanLeft”).
- House-Dog: “The scene shifts to a cozy, inviting living room, with a crackling fireplace and soft, comfortable seating.”
- Lib-Batman: “A gothic library with dark wood shelves and candlelight.”
- Winter-Cat: “A cat walks towards the camera in a snowy foresty, 8k uhd, soft lighting, high quality.” (MotionLora: “Zoom-In”).

The videos cover a variety of scenes, from indoor to outdoor, showcasing the diversity of the selected cases. We demonstrate the dynamics of the background by cropping clips at the same position from each original frame, as shown in Fig. 10. “Cabin-Dog” and “Lib-Batman” are two videos with relatively small background movement, where Cabin-Dog’s fireplace has a larger dynamic, creating a contrast with the surrounding static environment, while Lib-Batman’s scene has a high contrast of brightness and dark-

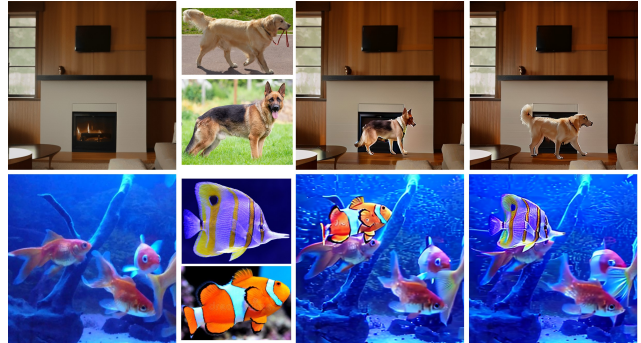


Figure 9. Visual examples of inserting different objects into the same scene, showing the robustness of DreamInsert.

ness. “Coffee-Bird” has complex smoke variations, while Crossing Man includes the movement of people and vehicles. “Hill-Horse”, “Forest-Horse” and “Winter-Cat” contain significant movements in the background, and accurately modeling these movements is difficult for video synthesis models.

Object Image. The object images in the cases cover animals and people including side and frontal perspectives. We chose them to better showcase both the motion creation after insertion and the reconstruction of interactions with the environment.

Regarding the selection of objects, unlike in 3D scene object insertion [22–24, 96], we did not choose still life or rigid body objects for demonstration. The main difficulty in 3D scene object insertion lies in rendering lighting and materials that correspond to the environment. In contrast, the challenges in I2V object insertion involve predicting the motion of static objects and reconstructing their environmental interactions. To verify the robustness of model, we prepare different objects for the same scene in “House-Dog” and “Gold-Fish”, resulting in 4 different cases. Visualizations are shown in Fig. 9.

Trajectory. We control the movement of the object through the trajectory, where the trajectory is generated by first giving the initial position and bounding box size, and then generating subsequent bounding boxes frame by frame according to different speeds, directions, and b-box size changes, and setting the value inside the bounding box to 1 and the value outside to 0.

1.2. Baseline Methods

To compare DreamInsert with existing object insertion methods, we choose three state-of-the-art content editing methods as baselines, containing training-based and training-free methods:

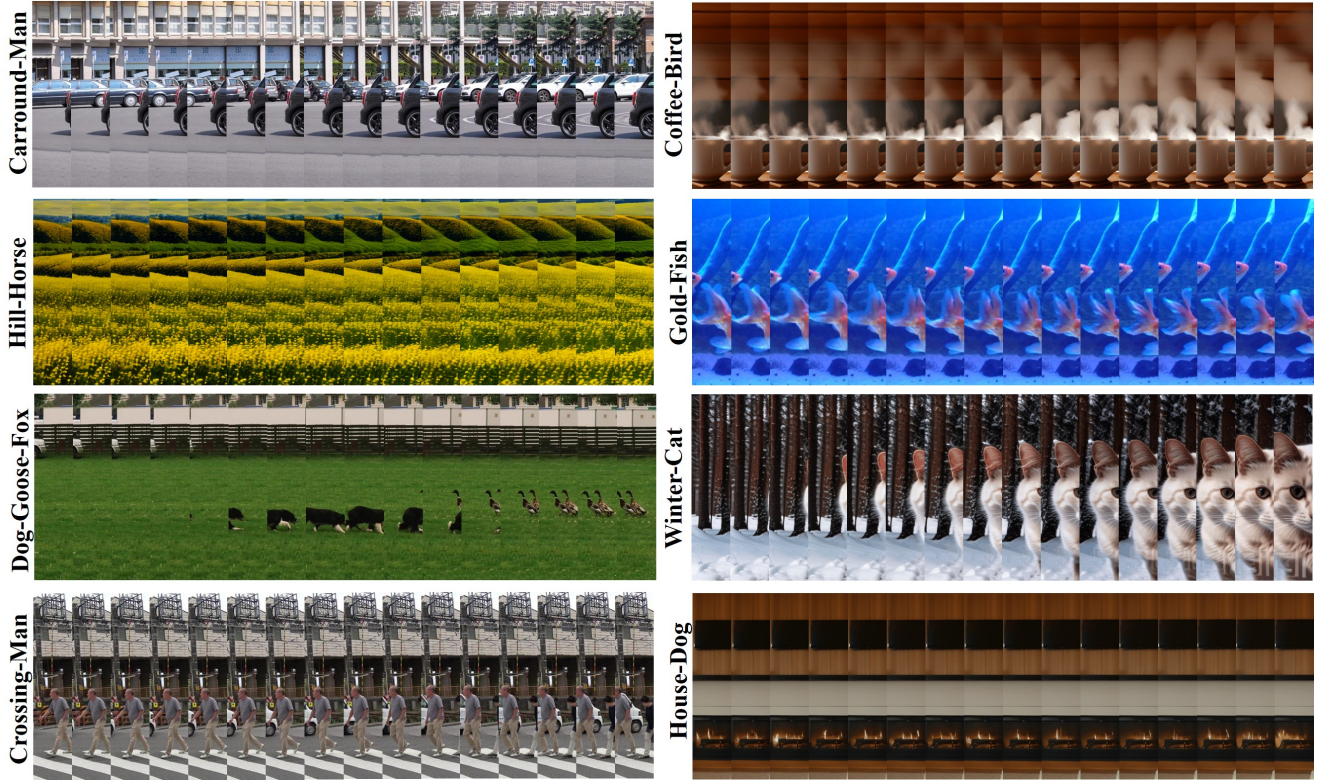


Figure 10. Visual examples of the background video used in I2VIns. Each clip is cut from the corresponding frame.

Training-Free Methods:

- **TF-ICON** [18] is an Image-to-Image (I2I) object insertion method that inserts an object from a given image into a target image using latent fusion. However, it does not perform well on realistic or natural images. We take the object image, trajectory frame, and background frame in the same timestamp as inputs and apply TF-ICON separately on each frame to obtain the synthesized result.
- **AnyV2V** [77] is an Image-to-Video (I2V) video editing method, achieves content editing using the first frame as guidance. However, AnyV2V only performs well in tasks such as style transfer or object replacement, and it is difficult for AnyV2V to predict the motion of unseen new objects. We copy the object to the target position following the trajectory to obtain the first frame, and the model uses prompt and the first frame as conditions to predict subsequent frames.

Training-based Methods:

- **CCEdit** [74] (Text-to-Video, T2V). We have adopted the official default model for CCEdit to control the insertion of objects through text. However, as CCEdit was not trained on the dataset for I2V target insertion, it is completely unable to perform such task. In practice, we take background video as input and attempt to add objects and their motion through text prompts.

We choose the above method to demonstrate the perfor-

mance of different existing pipelines on this problem. However, in fact, there is currently no method to achieve the I2V object insertion task because of the challenges mentioned in the main text, namely the lack of reference motion for static objects and the absence of image-video data pairs as training data.

2. Ablation Study

2.1. Motion Creation

We provide additional ablation study results to validate the effectiveness of the two stages processing in DreamInsert. We first validated the motion creation in the 1st stage. We compared the results obtained by synthesizing the latent domains (TF-ICON [18]), with motion created by DreamInsert. We input the former results into the model for subsequent alignment, and the results are shown in Fig. 11.

Comparing the results in the left column of Fig. 11 with those in Fig. 13 and Fig. 15, it can be seen that our proposed pixel-domain fusion can generate more diverse motions while preserving semantic consistency, resulting in better performance, while the output of TF-ICON, despite alignment, still cannot obtain motions consistent with the object.

Comparing the results in the right column of Fig. 11 with those in Fig. 21 and Fig. 14, it demonstrates the effectiveness of our proposed spatiotemporal alignment in the 2nd

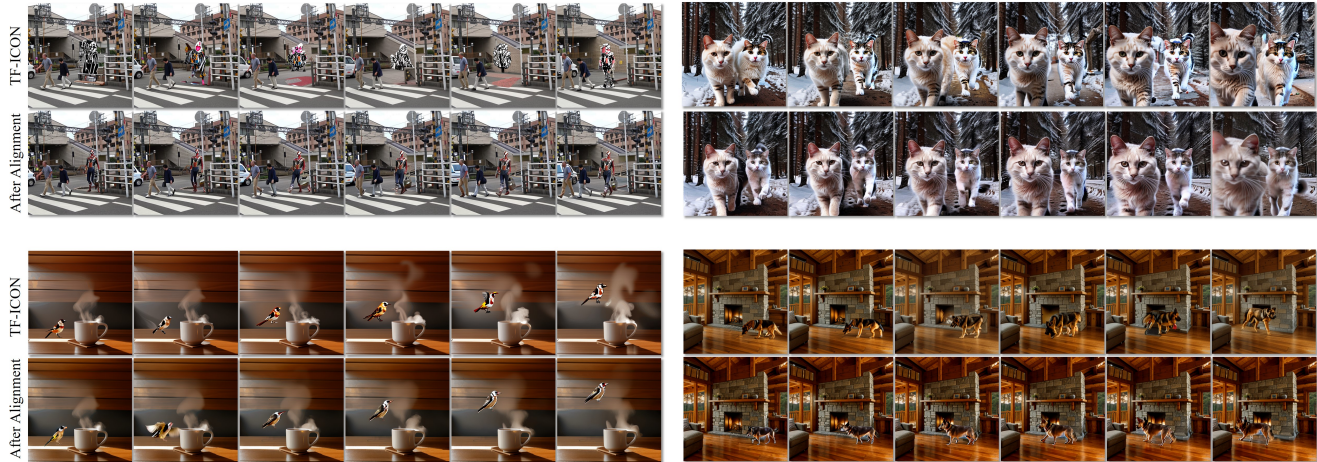


Figure 11. Ablation studies of motion creation in the 1st stage and spatiotemporal alignment in the 2nd stage. The top row in the left column indicates the effectiveness of motion creation in DreamInsert. Compared with the proposed motion creation, existing methods cannot generate motions for those difficult cases (Coffee-Bird and Crossing-Man), resulting in inconsistent object motions even after the alignment. The right-hand column reflects the effectiveness of spatial-temporal alignment in DreamInsert. For the Winter-Cat and Cabin-Dog, although there is still a certain gap between them and DreamInsert, the results of TF-ICON [18] are refined after the proposed alignment, indicating the effectiveness of proposed pipeline.

stage. For motion generated by latent-domain fusion that lacks consistency, alignment via the knowledge from I2V generation model can improve its consistency with objects.

2.2. Object Robustness

We design following experiment to verify the robustness of the model on different objects, as shown in Fig. 17 and Fig. 18. Among them, we kept the prompt, trajectory, and background video unchanged, and two completely different objects were inserted. Among them, Gold-Fish1 uses a clownfish with a significantly different appearance from the background, while Gold-Fish2 uses a blue fish that is very similar to the background. From the visualizations, it can be seen that due to the presence of fish of the same type as the new object in the background, it is difficult for the baseline method to correctly distinguish them, resulting in incorrect insertion results. Regardless of domain differences, DreamInsert achieved reasonable insertion results. D-Inv shows better robustness as it correctly models the spatial relationship between objects and background while keeping the fidelity.

3. Quantitative Comparison

We offer various quantitative comparisons among three aspects of **Fidelity**, **Text-Matching** and **Overall Quality**, to compare the performance between different methods on the I2VIns Dataset. We use Clip-I, Clip-T score [111], DINO Score [109] and Adv-Viclip score [105] as metrics. DreamInsert in both the PN-Inj and D-Inv settings achieves comparable results, showing its effectiveness.

3.1. Fidelity Comparison using Clip-I and DINO Score

Clip-I Score. We calculated the average Clip Image (Clip-I) score by comparing generated frames to the copied sequence to evaluate the faithfulness between the output and the original background and object. Maintaining the fidelity of the background is also important in I2V insertion. The results are presented in Tab. 3.

Clip-I Score	AnyV2V	CCEdit	TF-ICON	PN-Inj.	D-Inv.
Cabin-Dog	96.29	89.81	95.25	95.45	96.43
Carround-Man	86.77	70.74	87.64	86.27	85.67
Coffee-Bird	91.23	77.81	92.77	89.31	95.11
Crossing-Man	77.71	59.62	76.26	91.97	91.93
Dog-Goose-Fox	81.85	67.20	89.05	79.94	85.92
Forest-Horse	93.80	73.76	92.80	93.99	93.77
Gold-Fish1	91.80	80.64	89.04	94.52	91.17
Gold-Fish2	92.32	81.64	87.49	92.90	91.58
Hill-Horse	84.75	67.66	93.96	93.35	96.09
House-Dog1	89.95	64.15	90.25	92.48	92.27
House-Dog2	95.64	70.29	94.45	94.98	93.55
Lib-Batman	84.00	68.24	90.86	94.85	92.80
Lucia-Dog	82.37	63.44	86.92	83.71	82.86
Winter-Cat	93.62	75.73	95.99	97.15	95.69
Average	88.72	72.19	90.19	91.49	91.77

Table 3. Comparison of frame fidelity using Clip-Image Score.

DINO Score. In order to more accurately evaluate the fidelity of the inserted object, we follow the VBench [110] setting, using DINO score [109] as metric. We calculate the DINO score between the reference image and the bounding-box area of each synthesized frame. Differ from Clip-I score which measure the distance between two frames, DINO score calculates the object area between the object image and predicted frame, can more accurately evaluate the fidelity of the object itself.

DINO Score	AnyV2V	CCedit	TF-ICON	PN-Inj.	D-Inv.
Cabin-Dog	0.591	0.486	0.737	0.692	0.700
Carround-Man	0.682	0.601	0.690	0.657	0.693
Coffee-Bird	0.567	0.561	0.680	0.616	0.662
Crossing-Man	0.542	0.513	0.601	0.700	0.692
Dog-Goose-Fox	0.708	0.508	0.742	0.753	0.764
Forest-Horse	0.667	0.534	0.839	0.846	0.813
Gold-Fish1	0.843	0.715	0.646	0.852	0.813
Gold-Fish2	0.807	0.720	0.899	0.906	0.913
House-Dog1	0.575	0.470	0.695	0.605	0.645
House-Dog2	0.682	0.491	0.747	0.750	0.742
Hill-Horse	0.618	0.526	0.811	0.765	0.815
Lib-Batman	0.543	0.529	0.645	0.694	0.655
Lucia-Dog	0.639	0.514	0.732	0.725	0.755
Winter-Cat	0.578	0.587	0.828	0.840	0.860
Average	0.645	0.534	0.735	0.743	0.751

Table 4. Comparison of object fidelity using DINO score.

Results. As shown in Tab. 3 and Tab. 4, D-Inv achieves the best results (91.77 of Clip-I and 0.751 of Dino). DreamInsert achieved outstanding performance in maintaining the fidelity of both the background and object, with both settings outperforming baseline methods.

3.2. Text-Matching Comparison using Clip-T Score

We calculated the average Clip Text (Clip-T) score between each generated frame of each model’s output and the input text prompt, thereby gauging the accuracy of the created motions instructed by the text. The results are given in Table 5. PN-Inj achieves the best results, with D-Inv coming in second. The score of all methods on the Clip-I score is not high, because the prompt used in I2V insertion is intended to control the motion of the object and therefore does not include background description. The Clip-T score calculates the distance between each frame and the prompt separately, which introduces a certain degree of error. Nevertheless, under the same prompt, DreamInsert still achieves the best results, demonstrating that the generated motion is more in line with the prompt’s instructions.

Clip-T Score	AnyV2V	TF-ICON	CCedit	PN-Inj.	D-Inv.
Cabin-Dog	17.64	23.83	18.25	21.04	21.14
Carround-Man	24.91	18.97	25.82	25.42	25.01
Coffee-Bird	20.93	25.70	28.39	21.79	25.10
Crossing-Man	24.13	24.82	25.08	24.86	24.44
Dog-Goose-Fox	33.20	33.75	32.82	33.32	33.51
Forest-Horse	29.05	31.18	27.63	30.38	30.37
Gold-Fish1	28.22	29.20	27.86	28.26	28.17
Gold-Fish2	28.26	27.16	28.83	28.35	28.11
Hill-Horse	22.81	30.04	22.28	29.85	29.56
House-Dog1	21.32	17.58	18.96	21.66	21.62
House-Dog2	24.67	18.42	24.28	24.44	25.16
Lib-Batman	20.06	25.22	20.11	25.28	25.26
Lucia-Dog	26.72	23.88	28.14	26.79	26.34
Winter-Cat	28.95	30.12	29.42	29.95	29.71
Average	26.75	24.13	26.67	26.89	26.84

Table 5. Comparison of text-matching performance using Clip-Text Score.

Case	Prompt (<i>Top</i> : Optimal, <i>Bottom</i> : Fake)
Coffee-Bird	A bird flies slowly, head upward. A bird walks slowly to the top, head upward.
Cabin-Dog	A german shepherd walks to the left of the cabin. A german shepherd stands on the floor.
Crossing-Man	Three man walk through Two man walk through.
Forest-Horse	A horse walking slowly to the left. A horse walking around
Hill-Horse	Horse running Horse eating grass.
Lib-Batman	Batman walks into the room. Batman flies into the room.
Winter-Cat	Two cats walk towards the camera. One cat walks towards the camera.
House-Dog1	A german shepherd walks to the right of room. A german shepherd walks in the forest.
House-Dog2	A golden retriever walks to the right of the room. A golden retriever walks to the left of the room.
Dog-Goose-Fox	Fox chasing the goose. Fox chasing the goose and dog.
Carround-Man	A man walks next to a black car. A man driving the black car
Lucia-Dog	A woman walking the dog. A woman walking and dog stop.
Gold-Fish1	A clownfish swimming with other three fishes. Three clownfish are swimming.
Gold-Fish2	A blue fish swimming with other three fishes. A blue fish swimming with other two fishes.

Table 6. Adversarial Prompt list with optimal prompt on the top and fake one on the bottom.

Adv-Viclip	AnyV2V	CCedit	TF-ICON	PN-Inj.	D-Inv.
Cabin-Dog	0.960	0.801	0.990	0.991	0.992
Carround-Man	0.981	0.803	0.994	0.994	0.995
Coffee-Bird	0.525	0.740	0.762	0.745	0.743
Crossing-Man	0.150	0.418	0.379	0.274	0.443
Dog-Goose-Fox	0.771	0.838	0.930	0.793	0.860
Forest-Horse	0.827	0.001	0.841	0.804	0.900
Gold-Fish1	0.573	0.211	0.003	0.683	0.582
Gold-Fish2	0.530	0.017	0.685	0.393	0.590
Hill-Horse	0.686	0.001	0.959	0.976	0.953
House-Dog1	0.576	0.001	0.478	0.675	0.697
House-Dog2	0.524	0.043	0.643	0.490	0.426
Lib-Batman	0.602	0.335	0.664	0.727	0.835
Lucia-Dog	0.584	0.552	0.601	0.633	0.670
Winter-Cat	0.303	0.682	0.980	0.993	0.987
Average	0.613	0.388	0.707	0.726	0.763

Table 7. Comparison of overall quality using Adv-Viclip score.

3.3. Overall Quality Comparison using Adversarial Viclip Score

We use a pretrained large-scale video-text model, Vi-clip [105], to evaluate the overall consistency. Viclip is built upon Clip and consists of a video encoder (ViT) and a text encoder. Both modules are initialized from the corresponding Clip components. It incorporates both contrastive learning and masked modeling techniques, allowing for efficient learning of transferable video-language representations. We use Viclip to evaluate the insertion quality and propose the *Adversarial Viclip (Adv-Viclip) Score*.

In detail, we provide a list of optimal prompts, \mathbb{L}^{opt} , each corresponding to a case in the I2VIns dataset, which describes the ideal synthesis effect for that case. For the synthesis results obtained by different models, Viclip calculates the distance between the synthesis results and all the prompts in \mathbb{L}^{opt} and outputs the probability corresponding to each prompt. We take the probability value of the ground truth prompt as the result to evaluate the performance.

Due to the unique nature of the insertion task, calculating only the probability between the output video and the optimal prompt is insufficient to evaluate the performance. This is because the differences between each case can be quite significant, meaning that even if the insertion quality is not good enough, Viclip can still find the optimal prompt as the closest match with a high probability value. Therefore, we design a set of fake prompts, \mathbb{L}^{fak} . Compared to the optimal prompt, each fake prompt in \mathbb{L}^{fak} corresponds to one in \mathbb{L}^{opt} , describing the same case in I2VIns. However, the prompts in \mathbb{L}^{fak} describe failure situations of the case, emphasizing the difference between the good and fake ones. Viclip will search for the prompt that best matches the generated results from the combined list $\mathbb{L}^{\text{adv}} = \mathbb{L}^{\text{opt}} \cup \mathbb{L}^{\text{fak}}$, thereby providing a more accurate evaluation. For the final probability value which measured on \mathbb{L}^{adv} , we refer to it as Adversarial Viclip (Adv-Viclip) Score. All the results of different models using Adv-Viclip score are shown in Table 7, and the prompt list \mathbb{L}^{adv} is presented in Table 6.

4. User Study

We randomly selected 7 videos for the user study. 20 users evaluated the insertion performance of these 7 cases, each containing insertion results from 5 different methods. The evaluation indicators are divided into five aspects, namely Fidelity, Motion Smoothness, Environment Interaction, Text-matching, and Overall Quality. For each aspect, we pose a question and users rate it on a scale of 1 to 5 (Failed, Poor, Fair, Good, and Perfect). The five questions are as follows:

- *Fidelity*: Is the object in the synthesized video consistent with the object in the reference image?
- *Motion Smoothness*: Is the object’s motion in the video reasonable?
- *Interaction*: Is the integration and interaction of new objects with the surrounding background harmonious in composite videos?
- *Text-matching*: Does the synthesized video match the textual description provided?
- *Overall Quality*: What is the overall performance of the result?

Results. The evaluations of each video are given in Tab. 8. The average score of DreamInsert showed significant competitiveness, with PN-Inj receiving a score higher than 3 (“Fair”) compared to existing methods with a score close

Videos	AnyV2V	CCEdit	TF-ICON	PN-Inj.	D-Inv.
Cabin-Dog	2.99	1.35	1.96	3.40	3.83
Coffee-bird	2.24	1.31	2.89	2.69	3.91
Crossing-Man	1.71	1.41	1.45	3.96	3.79
Forest-Horse	2.36	1.13	2.49	3.64	4.08
Hill-Horse	2.25	1.08	2.09	3.20	3.93
Lib-Batman	2.01	1.12	1.99	4.01	4.31
Winter-Cat	2.24	1.32	2.28	4.28	4.17
Average	2.26	1.24	2.16	3.59	4.00

Table 8. User study comparison on different videos.

to 2 (i.e. evaluation of “Poor”), while D-Inv received an evaluation score 4, close to “Good”. Especially for the case of real videos like “Crossing-Man”, the scores for baseline methods did not reach “Poor”, while DreamInsert in two settings received ratings close to “Good”.

5. Case Study

In order to better demonstrate the insertion effect of DreamInsert and compare it with baseline models, we provide several case studies. The comparison results are shown in Figures 13–21 where detailed discussion of each case is presented in the caption. The top row is the background video, the red bounding box is the trajectory, and the top-right is the object image. The other rows are results obtained from different baselines, where “PN-Inj.” represents the results obtained by performing pixel-level noise injection and alignment, while “D-Inv.” is the default setting of DreamInsert, representing the results obtained by using motion creation and alignment. We presented the 2nd, 4th, 7th, 10th, 13th, and 16th frames of the output results (unless otherwise specified) of different methods for a fair comparison. In the rightmost column, we present the details of the synthesized object in the 16th frame, specifically to compare the spatial and temporal consistency among different methods.

Both the PN-Inj and D-Inv pipeline demonstrate certain effectiveness. While PN-Inj performs better for objects with little change in subject (such as the human body in Fig. 15 and Fig. 20, or objects in the frontal view of Fig. 21, etc.), as pixel-level noise injection does not significantly alter the spatial features and appearance of the object. The D-Inv pipeline shows its advantages in scenarios with significant changes in object appearance (horse in Fig. 19), where new actions that do not exist originally need to be added (e.g., bird flying in Fig. 13), or where the bounding box in the trajectory undergoes size changes and the interaction area is complex and varied (Fig. 16).

Failure Case Currently, all methods have poor insertion performance when the pixels of the object are limited. Fig. 12 shows a failure case where the model attempts to insert a person into the Carround video from DAVIS16 [107]. However, due to the small number of pixels occupied by the human face in the object image, the model finds it difficult

to extract its spatial features. Especially after $8 \times$ downsampling by the VAE in LDM [25], it is difficult for the model to reconstruct the face. All of the methods have shown blurred predictions. However, due to reasonable modeling of the motion, DreamInsert still achieved comparable results.

other generative model methodologies or content manipulation techniques. ongoing research in generative modeling, particularly personalized generative priors, must persist in examining and reconfirming these issues.

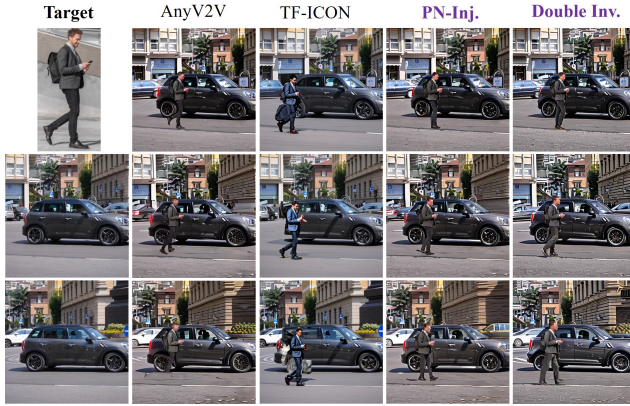


Figure 12. Blurring issue, using Carround-Man as a example.

6. Limitations

Currently, our method has achieved a preliminary breakthrough in I2V object insertion for specific scenarios, enabling the creation of coherent dynamic videos of certain durations. However, we face three major limitations: Firstly, the generation quality for human faces and bodies is moderate, due to humans’ heightened sensitivity to the authenticity of facial and bodily features [112], making it challenging to maintain consistency in real videos. Secondly, synthesizing long-term video sequences is difficult because the motion states of the static object become more complex and harder to predict them over extended periods in consistency. Thirdly, accurately preserving background details during object-environment interactions remains a significant challenge for all image and video editing and synthesis algorithms. We plan to delve deeper into these issues in our future research endeavors.

7. Social Impacts

Our original intention is to provide possibilities for film and television production [2], or to assist in psychotherapy [4], post-traumatic stress disorder (PTSD) treatment [113], etc., to reproduce the scenes in people’s memories, or to achieve the integration of imagined scenes. Current methods for object insertion in realistic videos struggle to produce coherent synthesized videos, whereas our method is capable of generating short-term videos with consistent motion, thereby opening up new creative possibilities for such video synthesis and editing tasks and serving as a catalyst for future research. However, malicious parties may use this technology to create false news or harmful video content to mislead viewers. This is a prevalent problem that also arises in

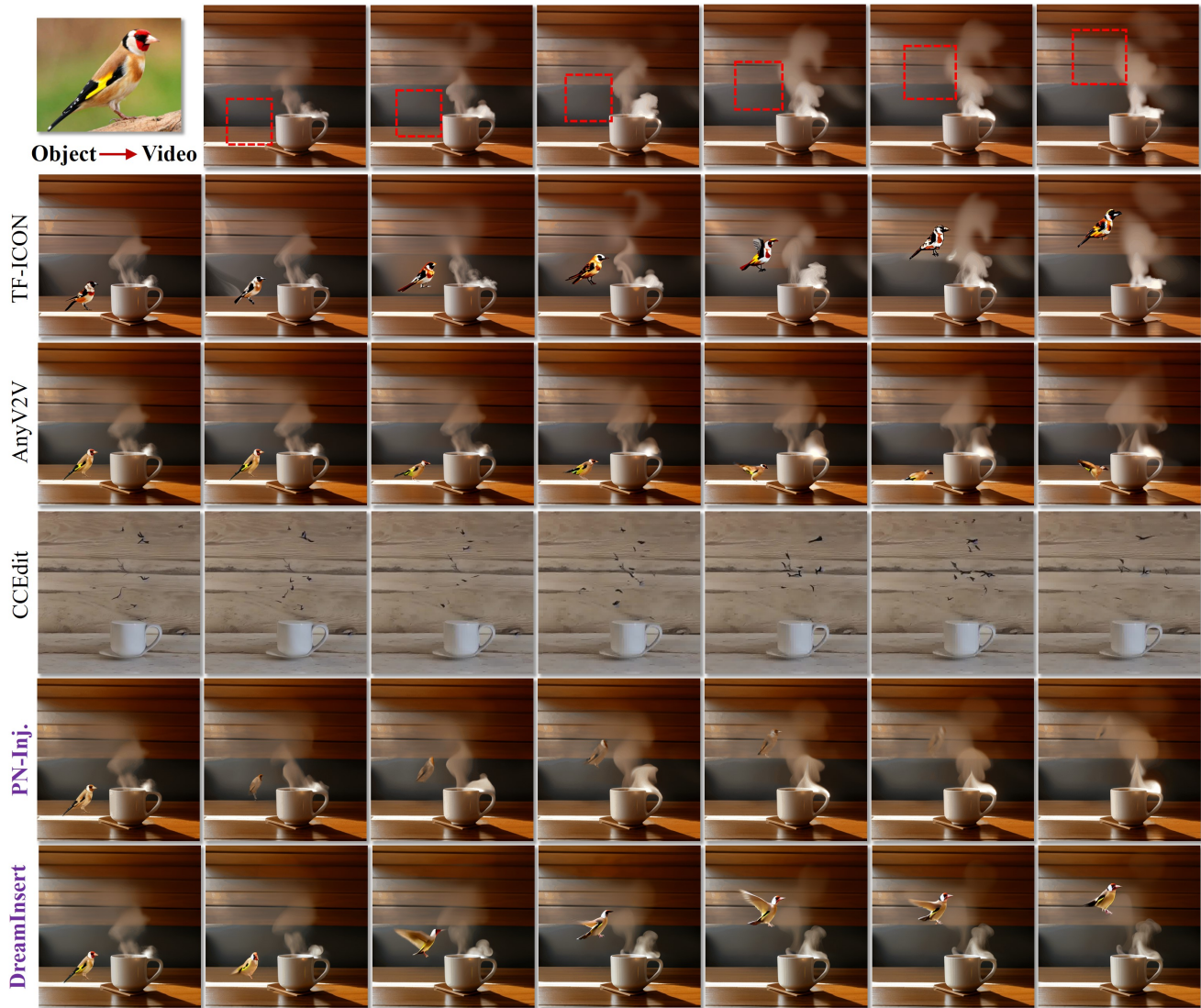


Figure 13. Visualized comparison on the Coffee-Bird. The Coffee-Bird is the most difficult scene because the bird in the object image lacks the conditions to fly at all, and even its wings are barely recognizable. Under the PN-Inj setting, it is also challenging to reconstruct non-existent flying actions using alignment in the second stage. Only by first performing motion creation and then aligning can a coherent and consistent bird flight video be generated, enabling the insertion of objects into a new scene. It is worth mentioning that, in the setting of a bird flying next to a coffee cup, it is nearly impossible to find relevant real videos as training samples. This indicates the novelty of DreamInsert, which can achieve zero-shot object insertion. (Text prompt: *A bird flies slowly, head upward.*)

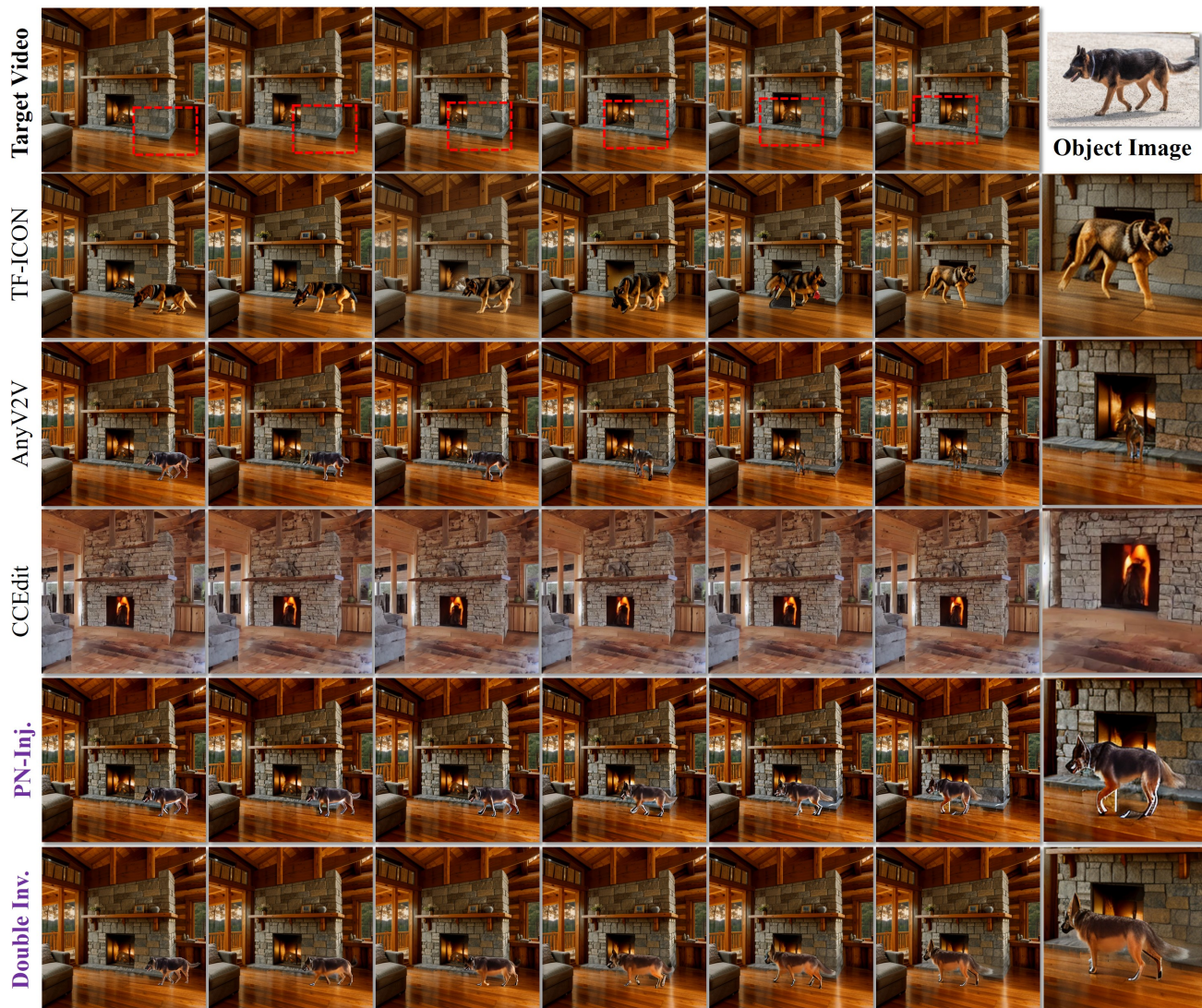


Figure 14. Visualized comparison on Cabin-Dog. Cabin-Dog is a relatively easy case, where both PN-Inj and D-Inv successfully generated coherent actions. However, D-Inv maintained better spatiotemporal coherence. TF-ICON [18] cannot understand the relationship between actions, scenes, and trajectories. Although AnyV2V [77] generates coherent actions, these actions do not conform to objective laws and cannot be precisely controlled. (Text prompt: *A german shepherd walks on the floor.*)



Figure 15. Visualized comparison on Crossing-Man. The main challenge of Crossing-Man lies not only in the fact that its background (bg) video is sourced from real videos (“Crossing”) in DAVIS16 [107], which are rich in details, but also in the fact that, due to the presence of other objects of the same category in the bg video, accurately controlling different objects within the same category poses a challenge for all models. DreamInsert achieved good results in both settings. The object vanishes completely in the second frame of AnyV2V [77]’s generation. TF-ICON [18] fails to even synthesize the object with the bg video, which underscores the effectiveness of our proposed pixel-level noise perturbation. In such scenarios, achieving precise synthesis and control of the object and bg frame in the latent domain, while maintaining spatiotemporal consistency across different frames, is almost impossible. (Text prompt: *A man walks through..*)



Figure 16. Visualized comparison on Forest-Horse. As mentioned in the main text, the major difficulty of Forest-Horse lies in the fact that the position and size of the bounding boxes in the trajectory change over time. Therefore, it is quite difficult to maintain the spatial consistency of objects, as the number and position of pixels they occupy are constantly changing. TF-ICON [18] fails to control the spatial coherence of objects in the latent domain, while AnyV2V [77] cannot control the movement of horses effectively, failing to generate coherent motion. When the bounding box size changes, PN-Inj struggles to balance the object and background in the interaction area. D-Inv, however, generates a coherent and consistent object motion. (Text prompt: *A horse walking slowly to the left.*)

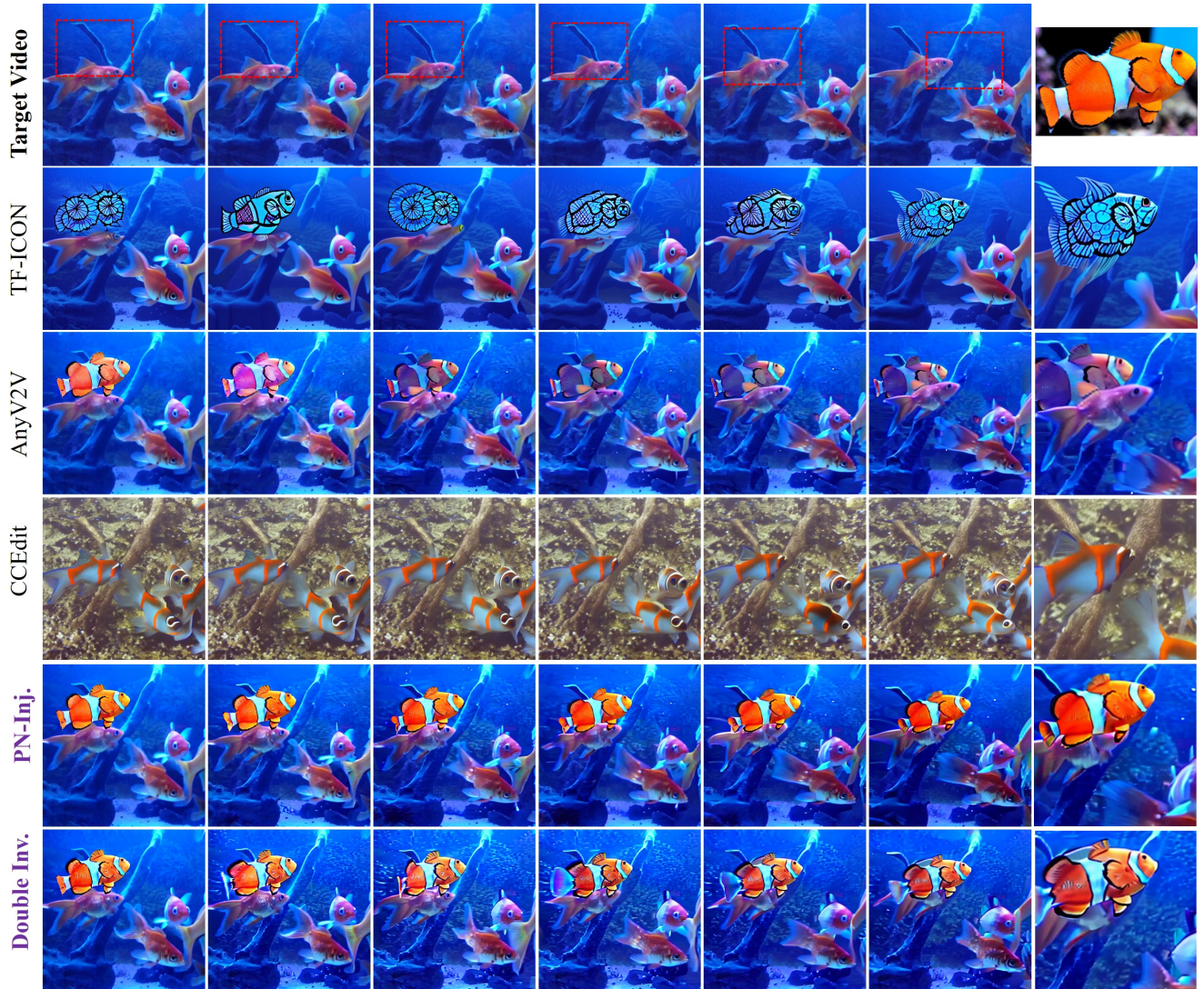


Figure 17. Visualized comparison on Gold-Fish1. The background video of Gold-Fish is from Davis16 [107], which depicts the scene of fish swimming underwater. In Gold-Fish1, we inserted a clownfish. The difficulty of this case lies in whether the model can reasonably maintain the appearance of the clownfish. AnyV2V [77] cannot reasonably maintain the appearance of the object, and the color of the clownfish in the first few frames has noticeably faded. When two fish were stacked, TFICON [18] can not understand the new object of clownfish and instead fused its appearance features with the background fish, generating an incorrect image. CCEdit [74] is unable to insert the object. Compared to PN-Inj, D-Inv not only maintains the fidelity of the object, but also better simulates environmental lighting and color, achieving the best results (Text prompt: *Fish Swimming.*)

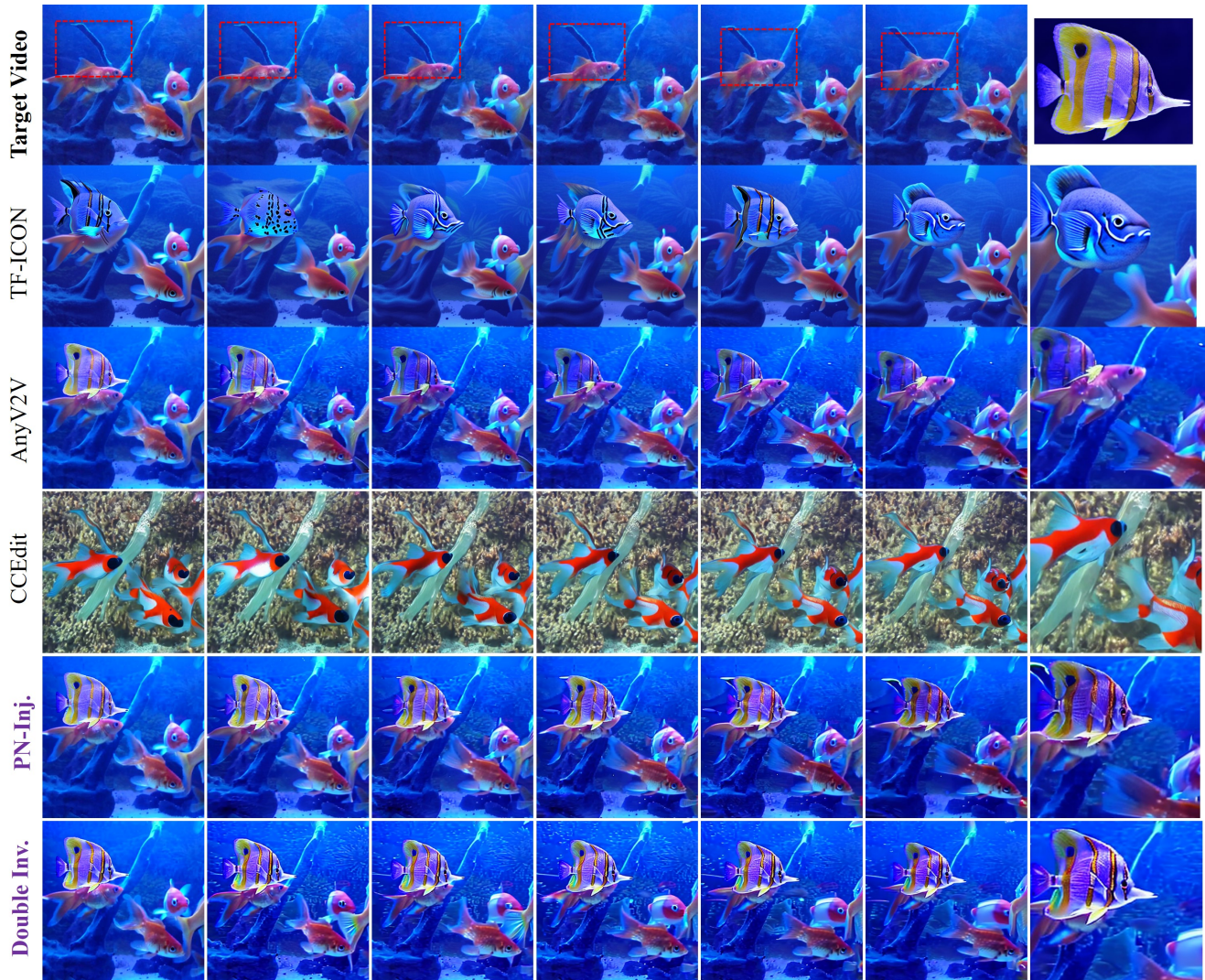


Figure 18. Visualized comparison on Gold-Fish2. In Gold-Fish2, we validated the ability to insert different objects in the same scene. We kept the prompt, trajectory, and background video unchanged, but changed the type of object. In this case, inserting a blue fish into the background is very difficult because the object’s color is similar to the background, making it easy for the model to confuse it with the environment. AnyV2V [77] cannot correctly distinguish objects, resulting in incorrect fusion of blue fish and background fish, and changing the appearance of the background fish without generating reasonable interaction between the object and the background. TFICON [18] has once again fused two fish, and CCEdit [74] is unable to insert objects. In the results of PN Inj, there were artifacts and distortions in the subsequent frame environment, while D-Inv achieved the best results, correctly modeling the spatial relationship between object fish and background fish while ensuring fidelity. (Text prompt: *Fish Swimming.*)

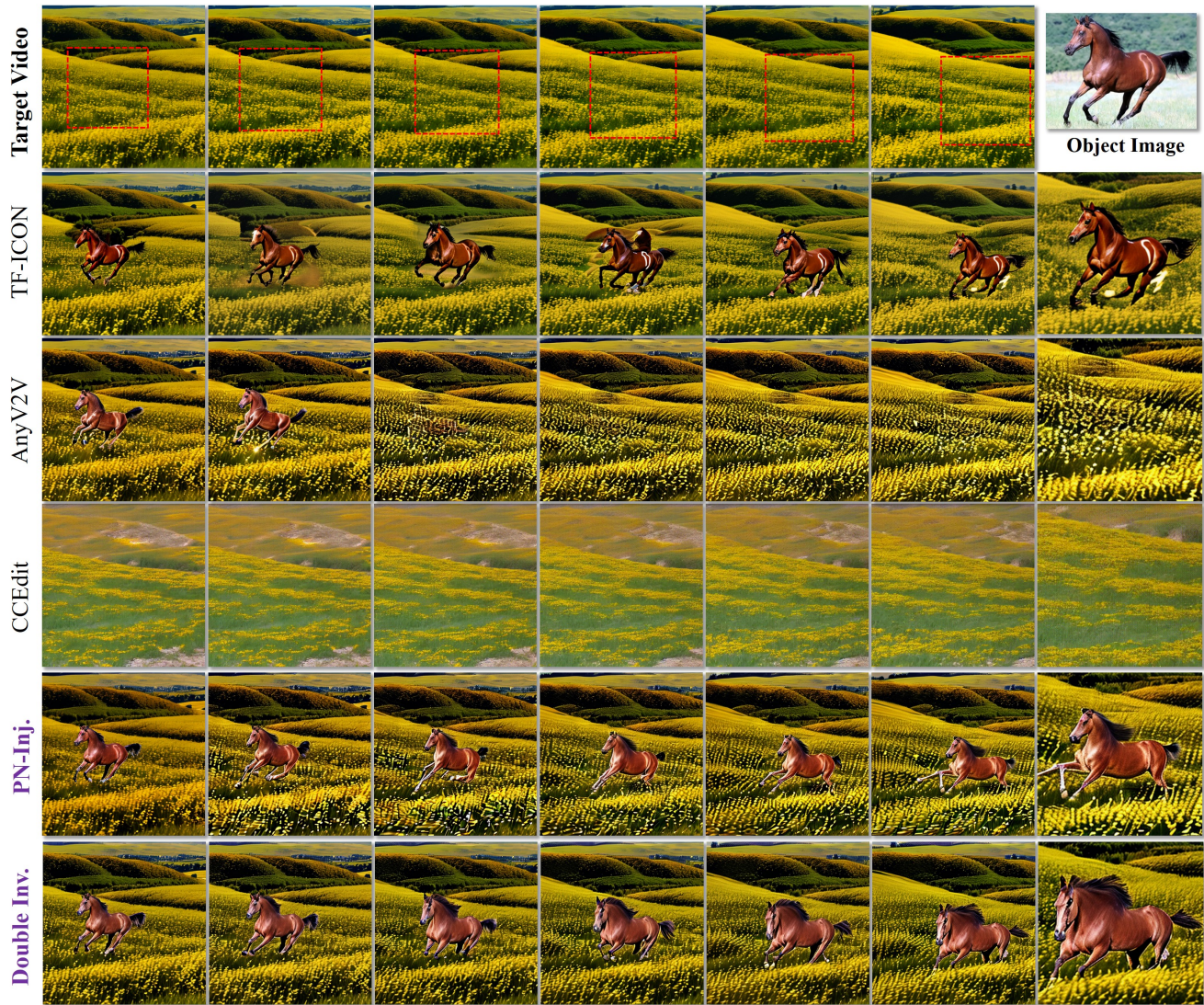


Figure 19. Visualized comparison on Hill-Horse. Also, it is very difficult to maintain consistency during the large movements of both object and background scene. The results of TF-ICON [18] are spatially and temporally incoherent. Due to the significant dynamics of the background, the object vanishes after the first five frames of AnyV2V [77]. PN-Inj struggles to maintain the relationship between legs and body due to the large dynamics of the scene and the intense object motion. D-Inv generates coherent and consistent object synthesis results, achieving the insertion of moving objects in large dynamic scenes. (Text prompt: *Horse running.*)

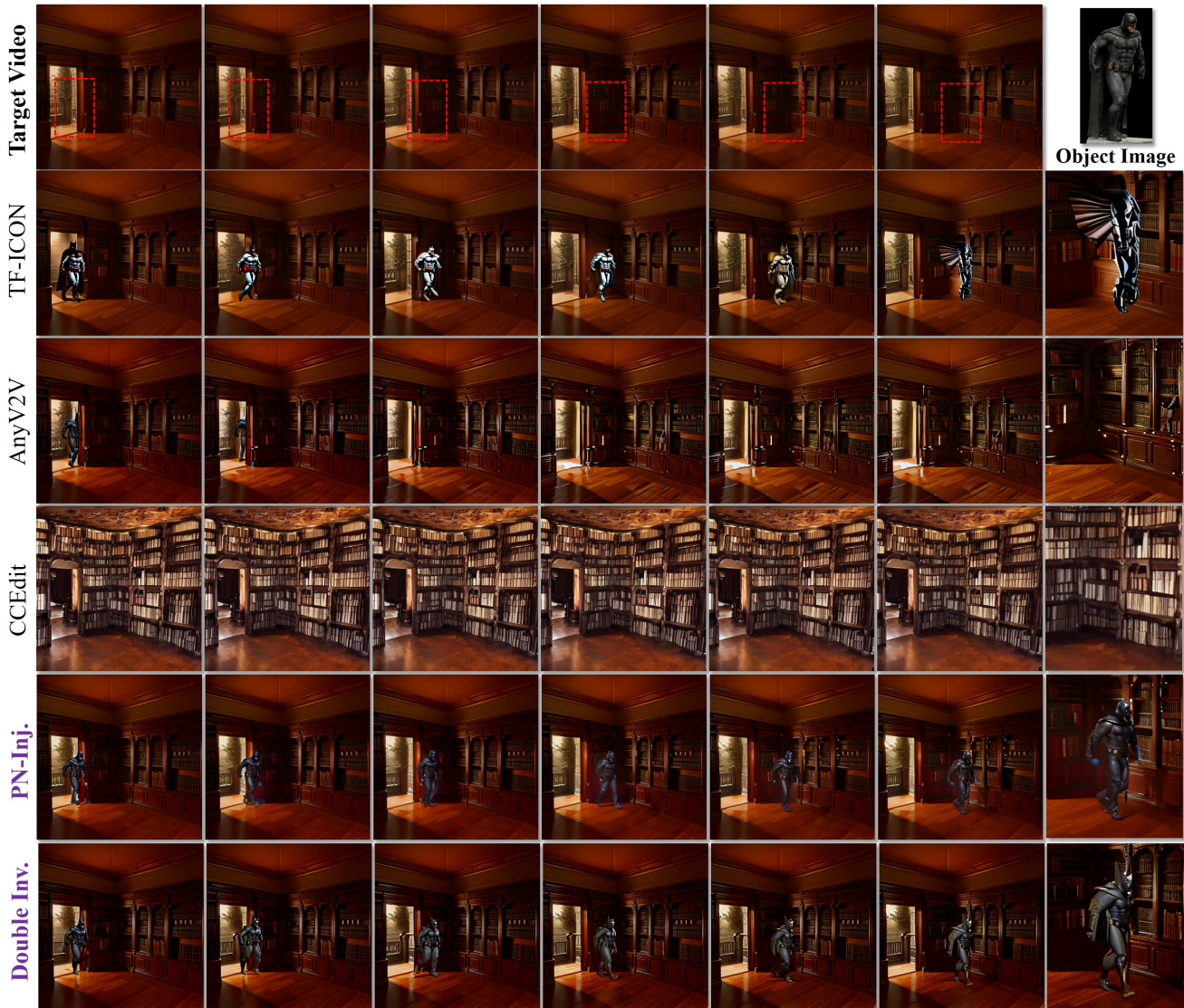


Figure 20. Visualized comparison on Lib-Batman. The difficulty of Lib-Batman lies in the fact that both objects and scenes are dim and dark, making it difficult to maintain spatial coherence of objects. TF-ICON [18] cannot maintain the consistency of objects, and AnyV2V [77] objects disappear in a short period of time. In this scenario, PN-Inj achieved better results because it maintained the consistency of the object subject. And based on the setting of motion creation, the object was reconstructed with bias. (Text prompt: *Man walking inside.*)

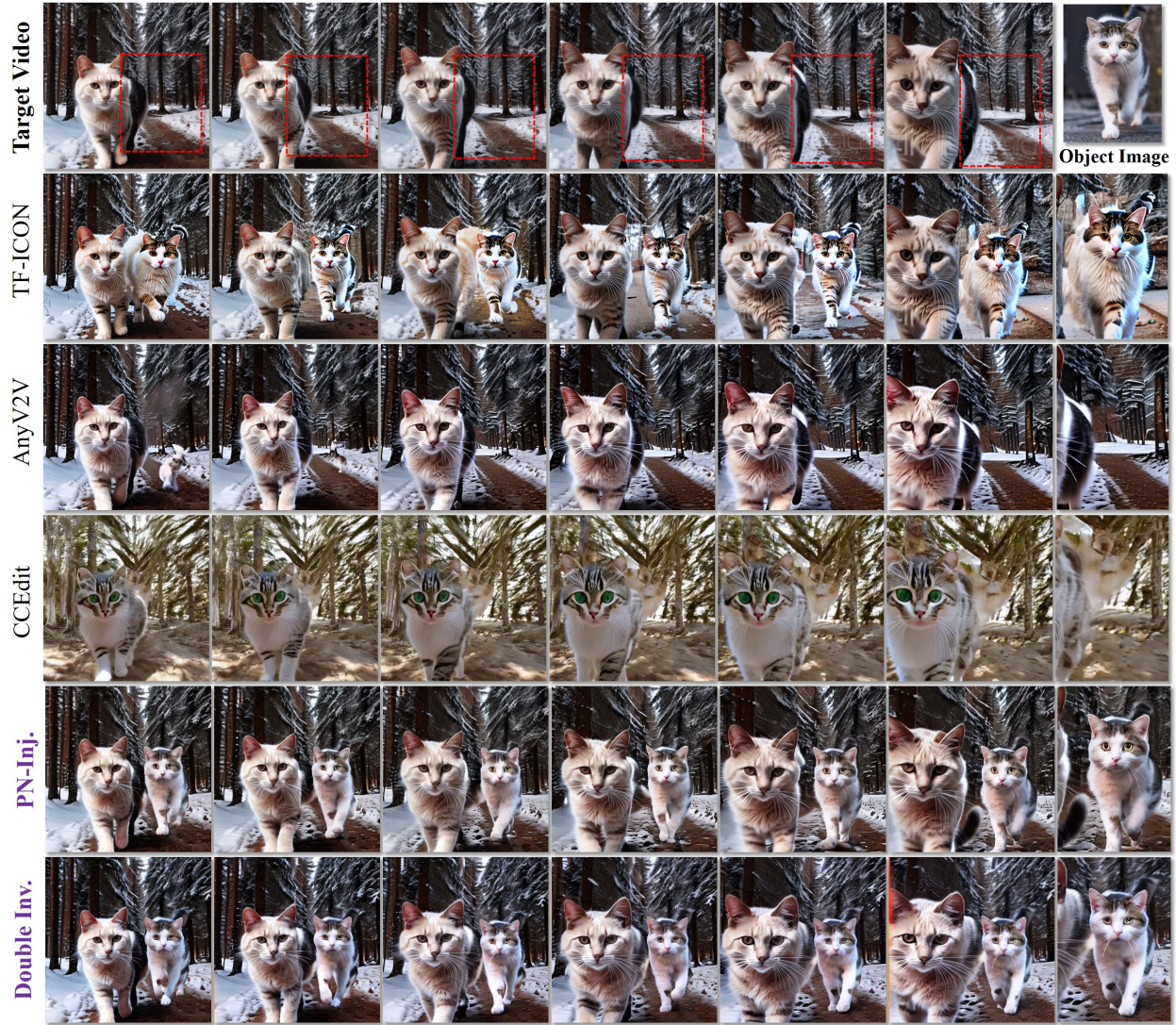


Figure 21. Visualized comparison on Winter-Cat. Winter-Cat is also a very difficult example, and its difficulty lies in: 1. The inserted object occupies a large proportion of the frame and requires consistency in its facial details; 2. The background image has significant dynamic (Zoom-In); 3. The category of the inserted object is the same as that of the original object. TF-ICON [18] inserted different cats frame by frame, and the cats in AnyV2V [77] disappeared within 3 frames. PN-Inj generated better insertion results, perfectly preserving the original characteristic of the cat’s face and producing coherent walking movements. (Text prompt: *Cat walk towards the camera.*)